

Engineered Biocatalysts for the Asymmetric Synthesis of D-Phenylalanines

Raluca Bianca Tomoiagă, Levente Csaba Nagy, Krisztina Boros, Mădălina Elena Moişă, and László Csaba Bencze*



Cite This: *ACS Catal.* 2025, 15, 7361–7389



Read Online

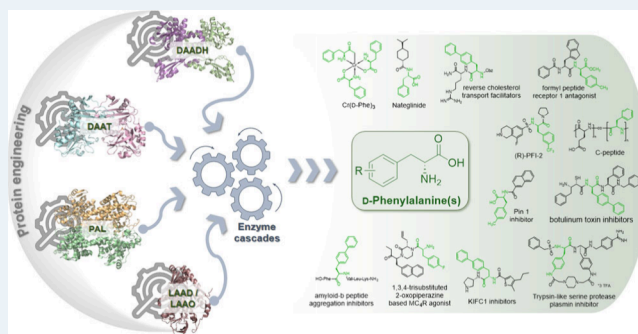
ACCESS |

Metrics & More

Article Recommendations

ABSTRACT: The enzymatic synthesis of D-phenylalanines, important chiral building blocks for several pharmaceuticals and fine chemicals, has been widely explored. Their asymmetric synthesis of high atom economy and accessible prochiral starting materials is highly attractive, while the expanding toolbox of protein engineering facilitates access to biocatalysts tailored for these processes. Accordingly, this Review provides an overview of the protein engineering efforts of enzymes involved in the asymmetric synthetic pathways for D-phenylalanines. The engineering efforts on D-amino acid dehydrogenases, D-amino acid transaminases, and phenylalanine ammonia-lyases to produce D-phenylalanines are thoroughly examined, while their application in (chemo)enzymatic cascades is also discussed. For an improved efficiency of the cascades, the protein engineering of L-amino acid deaminases and/or L-amino acid oxidases for an increased transformation of phenylalanines is also addressed.

KEYWORDS: D-phenylalanines, enzymatic asymmetric synthesis, protein engineering, D-amino acid dehydrogenases, D-amino acid transaminases, L-amino acid deaminases, L-amino acid oxidases, phenylalanine ammonia-lyases



1. INTRODUCTION

D-Phenylalanines are highly valuable chiral building blocks in the synthesis of several pharmaceuticals, including antibiotics, chemotherapeutic agents, peptides, and peptidomimetics (Figure 1).¹ Accordingly, D-Phe is a key component of polymyxins,² gramicidin S³ antibiotics, or of compounds with antidiabetic activity, such as nateglinide,⁴ C-peptides,⁵ and their chromium complex [Cr(D-Phe)₃].⁶ D-3-Trifluoromethylphenylalanine is an essential intermediate for (R)-PFI-2,⁷ an inhibitor for the SET domain containing lysine methyltransferase 7, involved in cancer-related signaling pathways. D-4-Methylphenylalanine is incorporated into Pin1 inhibitors⁸ and anti-inflammatory formyl peptide receptor 1 antagonists.⁹ D-Biarylalanines are intermediates for inhibitors of botulinum toxin,¹⁰ kinesin-14 motor protein KIFC1,¹¹ and amyloid- β peptide aggregation.¹² Cyclic plasmin inhibitors with high selectivity over related trypsin-like serine proteases can be synthesized using D-4-nitrophenylalanine as precursor,¹³ whereas D-4-fluorophenylalanine, upon incorporation, increased the binding affinity and agonist potency of 1,3,4-trisubstituted 2-oxopiperazine-based melanocortin-4 receptor agonists, potential antiobesity agents.¹⁴

For the synthesis of D-amino acids, including D-phenylalanines, biocatalytic methods have emerged as powerful synthetic procedures. Besides the established enzymatic kinetic

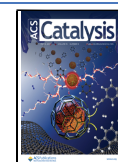
resolutions, yielding D-amino acids or their derivatives from their racemic mixtures with a maximal theoretical yield of 50%, procedures with improved yields and productivities have been developed. These include dynamic kinetic resolutions, coupled deracemization-stereoinversion methods or asymmetric synthesis, well summarized and/or reviewed in several reports.^{15–19} The expansion of directed evolution and metagenomic approaches highly facilitated the access to engineered and novel enzymes with significantly improved catalytic properties, also in the field of asymmetric synthesis of D-phenylalanines. In this Review, we present the advances within the field of enzymatic asymmetric synthesis of D-phenylalanines with a special focus on enzyme engineering and discovery efforts providing improved biocatalysts and synthetic procedures. While prior reviews within this topic^{15,17,19} largely focused on presenting the enzymatic pathways leading to D-amino acids and their fundamental aspects, we highlight and provide structural and/or mechanistic facets of the protein

Received: January 31, 2025

Revised: March 10, 2025

Accepted: March 17, 2025

Published: April 18, 2025



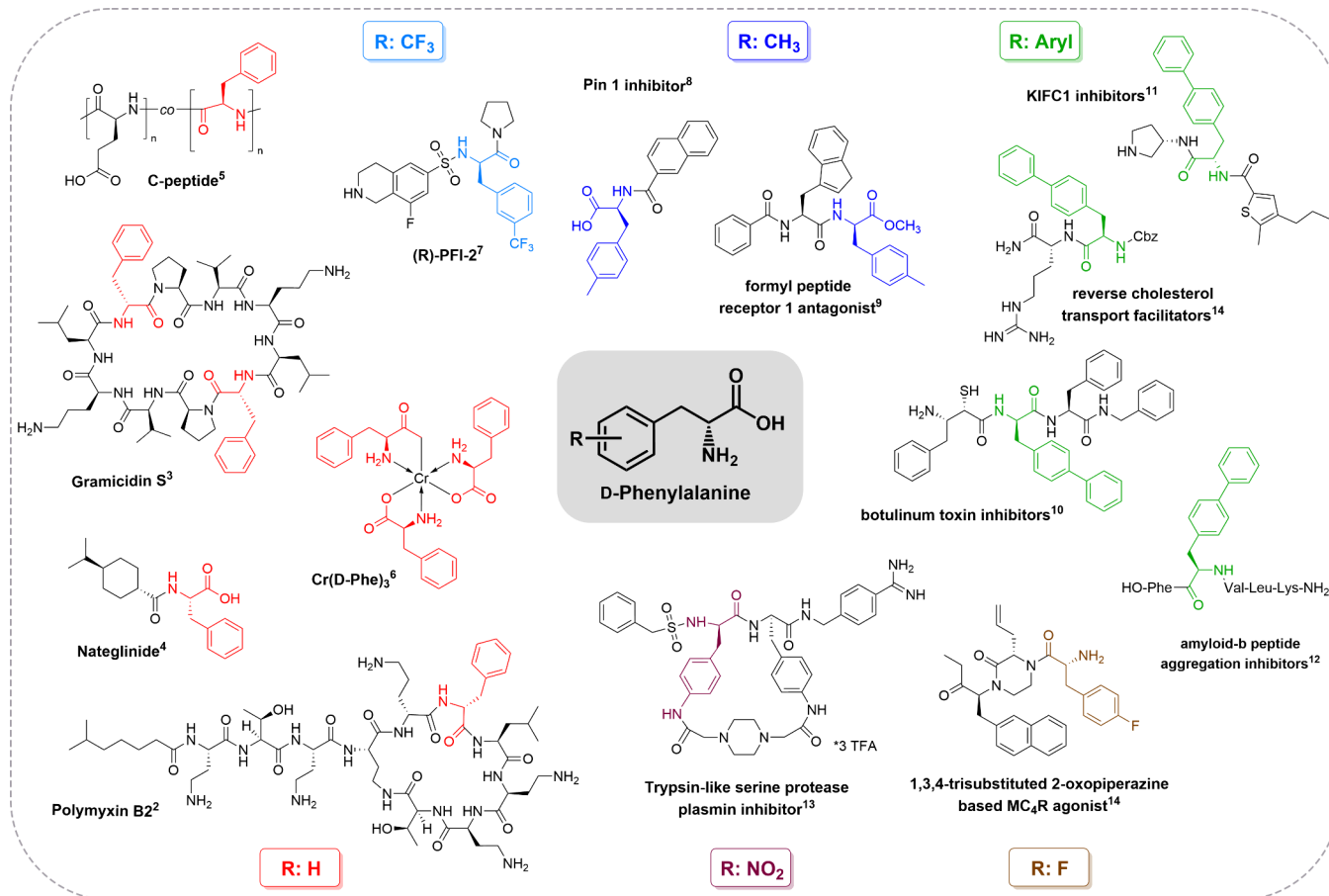


Figure 1. D-Phenylalanines as chiral synthons for APIs.

engineering efforts, delivering molecular level insights for the improved catalytic properties of the D-Phe-producing enzymes. Our approach provides a distinctive perspective by integrating the mechanistic understanding and molecular level rationale of protein engineering with practical synthetic applications. Notably, while strictly reviewing the asymmetric synthetic procedures, other, highly efficient, D-Phe producing biosynthetic procedures of industrial applicability, such as the hydantoinase–carbamoylase dynamic kinetic resolution,^{18–20} are not covered within this work.

2. ASYMMETRIC REDUCTIVE AMINATIONS BY ENGINEERED D-AMINO ACID DEHYDROGENASES

While amino acid dehydrogenases (AADHs) acting on L-amino acids are ubiquitous in nature, AADHs of opposite, D-selectivity have only been observed in a limited number of bacterial species, including *Pseudomonas aeruginosa*,^{21,22} *Pseudomonas fluorescens*,²³ *Pyrobaculum islandicum*,²⁴ *Salmonella typhimurium*,²⁵ and *Escherichia coli*.^{26–28} Moreover, AADHs preferentially catalyze the oxidative deamination route, while the occurrence of the reverse reductive amination reaction of α -keto acids, suitable for the synthesis of D-amino acids, has not yet been reported within living systems. To create an AADH of D-selectivity (DAADH) and broad substrate tolerance for the reductive amination of α -keto acids, two protein engineering strategies might be considered: (i) the reversal of the enantioselectivity of ubiquitous L-AADHs and/or (ii) the expansion of the substrate scope of other dehydrogenases that already possess the desired D-

selectivity. While protein engineering for enantioselectivity reversal has been successful in some cases,^{29–32} the absolute selectivity reversal is still considered highly challenging. Following the second, more facile engineering strategy, the *meso*-2,6-diamino-pimelic acid D-dehydrogenase (DAPDH, EC 1.4.1.16) of strict substrate specificity and low activity toward D-Phe, was selected to be engineered into a DAADH of broad substrate tolerance.³³ DAPDH catalyzes the reversible oxidative deamination of (R)- (or D)-amine of *meso*-2,6-diaminopimelic acid (DAP) giving L-2-amino-6-oxopimelic acid (L-AOP) while using NADP(H) as an electron acceptor/donor (Figure 2). A key feature of DAPDH is its ability to

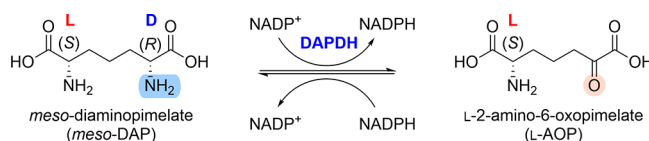


Figure 2. Oxidative deamination of *meso*-DAP and the reductive amination of L-AOP catalyzed by diaminopimelate dehydrogenase (DAPDH).

distinguish between the D- and L-stereocenters of *meso*-DAP, possessing D-selectivity.³⁴ In nature, the enzyme is involved in the biosynthesis of *meso*-DAP, which is found restrictively in bacteria, plants and fungi and provides L-Lys upon its decarboxylation.³⁵

Through phylogenetic analysis, 941 bacterial DAPDH sequences were differentiated into two classes: type I (68%

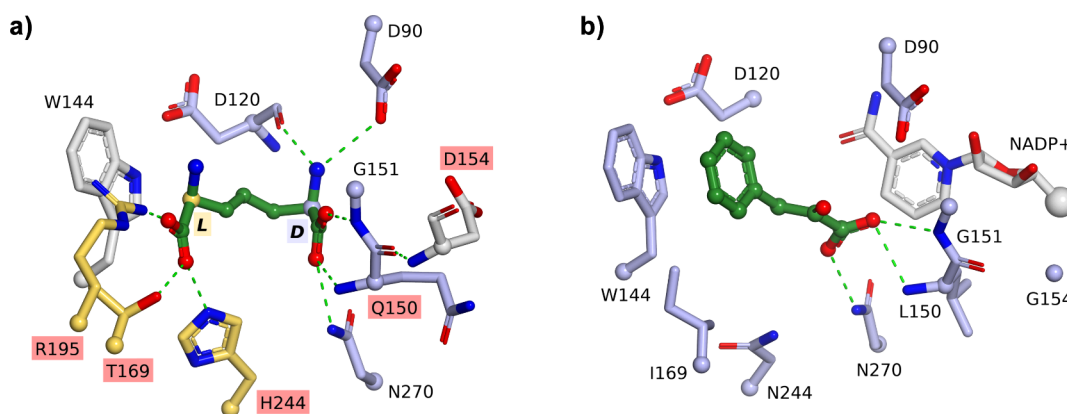


Figure 3. (a) The catalytic site of CgDAPDH accommodating *meso*-DAP (PDB: 2DAP), highlighting residues involved in the fixation of L- and D-stereocenters (marked in yellow and blue, respectively) and residues of which mutations provided the engineered CgDAADH (marked with highlighted labels); (b) The catalytic site orientation of the docked phenylpyruvate within the cofactor-bound structure of the engineered CgDAADH (PDB: SLOA).

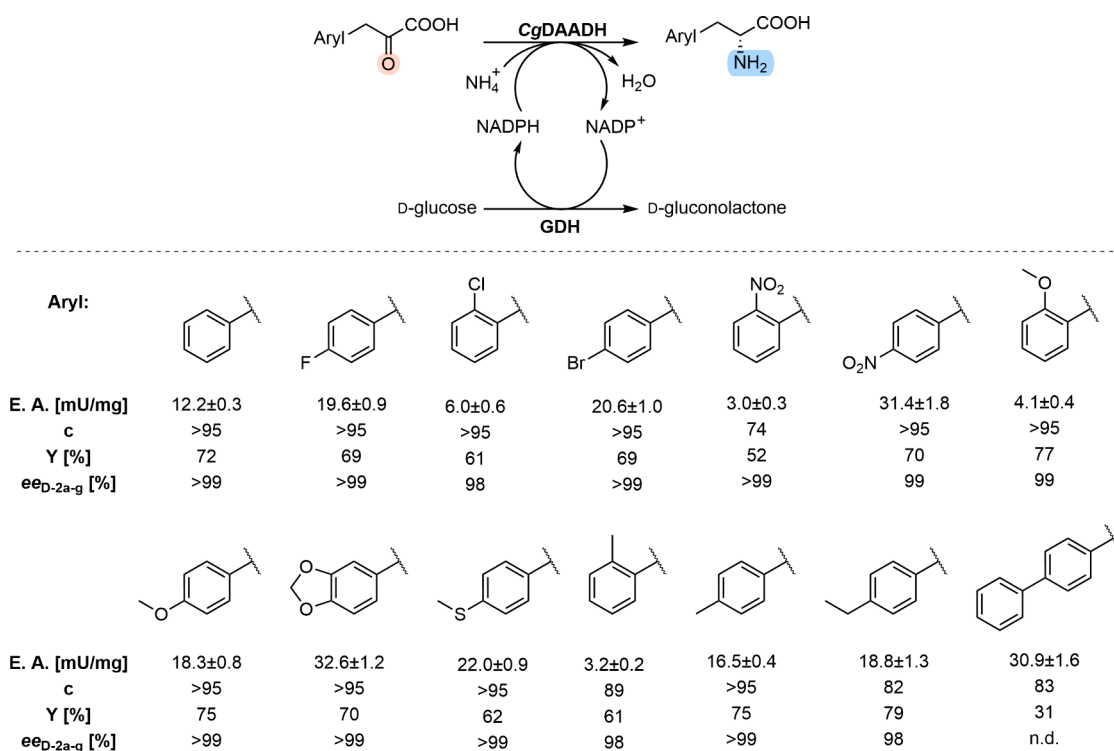


Figure 4. Tested aromatic substrate scope of the engineered CgDAADH: specific activity values were determined by using purified CgDAADH, while D-phenylalanines were produced with high enantiomeric excess (*ee*) and high isolation yields (*Y*) by using whole-cell biocatalysts co-expressing both CgDAADH and GDH. The figure was adapted with permission from ref 39. Copyright 2016 John Wiley and Sons.

of sequences) with high substrate specificity toward *meso*-DAP and no ability toward the reductive amination of 2-keto acids other than L-AOP and type II (32% of sequences) showing broader substrate tolerance in the reductive amination route.³⁶ Initially, for the directed evolution of DAPDH into DAADH,³³ the type I DAPDH from *Corynebacterium glutamicum* served as a template, benefiting from an established recombinant expression system³⁷ and structural data.³⁸ The saturation mutagenesis of residues R195, T169, and H244 of CgDAPDH, that interact with the L-stereocenter of DAP (Figure 3a), combined with error-prone PCR, provided variant Q150L/D154G/T169I/R195M/H244N, of significant activity in the reductive amination of diverse aliphatic and aromatic 2-keto acids, with D-Phe, D-*p*-Cl-Phe, and D-*p*-Br-Phe among the

products obtained.³³ While the engineered variant showed no activity toward the natural substrate, *meso*-DAP, it represented the first DAADH suitable for the production of various D-amino acids. The loss of its native activity can be attributed to mutations R195M, T169I and H244N, that strongly alter the active site fixation of the carboxylate from the L-stereocenter of DAP. In particular, mutations R195M and T169I facilitate the accommodation of D-amino acids with less polar side chain in comparison to *meso*-DAP. The error-prone PCR-derived mutations Q150L and D154G are positioned within the H-bonding network responsible for the fixation of the carboxyl group of the D-stereocenter, which consists of N270, Q150, G151, and D154 (Figure 3a).

Parmegianni et al.³⁹ tested the aromatic substrate scope of CgDAADH using whole-cell biocatalysts, also coexpressing glucose dehydrogenase (GDH) for cofactor regeneration. The preparative-scale reductive aminations provided valuable D-Phe analogues with high enantiopurities and excellent isolation yields in case of *para*- and/or *meta*-substituted derivatives, while moderate yields were registered for the *ortho*-substituted products (Figure 4).³⁹ Molecular docking of the aromatic 2-keto acids into the cofactor-bound structure of CgDAADH (PDB: SLOA) revealed polar interactions of the carboxylate and the keto group, similar to those observed for the D-stereocenter of *meso*-DAP (PDB: 2DAP). However, due to the Q150L mutation, the substrate's carboxylate group forms hydrogen bonds to the backbone amide of L150 (Figure 3b).³⁹ The loss of the polar interactions around the L-stereocenter of *meso*-DAP through mutations T169I, R195M, and H244N increases the hydrophobicity of this binding region, while I169 and W144 provide hydrophobic interactions with the substrate's aromatic moiety. This aromatic stacking interaction is considered to be responsible for the activity differences of substrates with different aromatic substitution patterns. The *para*- and *meta*-substituents enhance the overlap between the substrate's π -system with the indole ring of W144, thereby increasing the binding affinities. In contrast, *ortho*-substituents hinder this overlap, resulting in decreased binding affinity.³⁹

Additionally, CgDAADH was employed for the assembly of (chemo)enzymatic cascades, yielding D-phenylalanines (see Section 5.3).

To provide DAADHs of increased thermostability, mutations of the engineered CgDAADH were employed on homologue residues of DAPDH originally from *Ureibacillus thermosphaericus*, a thermophilic bacterium from Japanese compost, resulting in the creation of *UtDAADH*.⁴⁰ Classified as type I DAPDH, the enzyme maintained its activity operating at temperatures ~ 60 °C, demonstrating superior thermostability to CgDAADH, which loses activity at temperatures exceeding 48 °C.³⁷ The D94A variant of *UtDAADH* showed an 8.5-fold increase in catalytic efficiency ($k_{\text{cat}}/K_{\text{M}}$) within the reductive amination of phenylpyruvate (Table 1).⁴¹ The additional mutation Y224F did not affect enzyme activity,⁴¹ but the structure of variant D94A/Y224F *UtDAADH* (PDB: 5GZ6) revealed insights for the beneficial effect of mutation D94A. For DAPDHs and, accordingly, also for DAADHs, an ordered kinetic mechanism is plausible,⁴² wherein NADP⁺ cofactor binds first, followed by substrate binding, which triggers domain closure and initiates catalysis. By overlaying the closed, 2-keto-6-aminocaproic acid (KACA)-bound, subunit of D94A/Y224F *UtDAADH* (PDB: 5GZ6), with its open, NADP⁺-bound counterpart (PDB: 5GZ3) (Figure 5a) and comparing it with the similar overlay of the closed (both ligand- and cofactor-bound) and open (only cofactor-bound) subunits of CgDAPDH (PDB: 3DAP) (Figure 5b), differences in the relative positioning of conserved residues D94 and Y224 are revealed.

These suggest partial or incomplete domain closure within the ligand-bound structure of *UtDAADH* (PDB: 5GZ6). The closure of CgDAPDH implies the repositioning of the G151-G161 α -helix due to the formation of a salt bridge between D71 and R158. Concurrently, the H-bonding between Y219 and D90, homologous to that between Y224 and D94 from *UtDAADH*, repositions the T215-E224 loop (Figure 5b). This latter H-bond is also part of the H-bonding network involving S68 and the ribose unit of the NADP⁺ cofactor. In comparison,

Table 1. Summary Table with Reported Enzyme Activities and Kinetic Parameters of the Different DAADHs within the Reductive Amination of PPA

enzyme		reductive amination ^a		
		SA ^b (U/mg)	K _M (mM)	k _{cat} (s ⁻¹)
<i>LfDAPDH</i>	wild-type ^{c,50}	0.035	7.61	0.15
<i>CtDAPDH</i>	wild-type ^{c,48}	n.d.	n.d.	n.d.
	Q154L/T173I/R199M/ P248/H249N/N276S ^{c,48}	0.112	—	—
<i>UtDAPDH</i>	wild-type ^{c,40}	0.042	—	—
<i>UtDAADH</i>	wild-type ^{c,41}	0.235	—	—
	wild-type ^{d,41}	1.93	3.89	2.24
	wild-type ^{c,45}	2.46	1.50	—
	V137I/F306W/G311I/ S314L ^{c,45}	2.47	1.00	—
	D94A ^{d,41}	16.1	11.10	55.3
	Y224F ^{d,41}	1.67	—	—
<i>CgDAPDH</i>	wild-type ^{d,33}	n.d.	—	—
	wild-type ^{d,39}	0.012	—	—
<i>StDAPDH</i>	wild-type ^{c,51}	0.07	12.50	0.11
	wild-type ^{c,52}	0.01	—	—
	W121L ^{c,52}	0.98	—	—
	T171H ^{c,52}	0.91	—	—
	H227I ^{c,52}	2.41	—	—
	H227V ^{c,52}	2.40	24.30	3.98
	H227V ^{c,51}	0.46	—	—
	W121L/H227I ^{c,52}	4.96	12.20	6.20
	T171P ^{c,51}	0.15	15.80	0.53
	T171S ^{c,51}	0.19	19.60	0.88
	R181F ^{c,51}	0.44	11.10	1.07
	H227C ^{c,51}	1.03	15.50	2.48
	T171S/H227C ^{c,51}	0.74	13.90	2.37
	R181F/H227V ^{c,51}	1.35	20.80	3.43
	T171S/R181F ^{c,51}	0.28	13.90	0.70
	T171S/R181F/H227V ^{c,51}	1.02	11.00	2.09
<i>PvDAPDH</i>	wild-type ^{d,53}	0.08	4.95	0.19
	wild-type ^{d,54}	0.30	6.08	0.14
	WA21A ^{d,53}	—	6.19	2.19
	T171L ^{d,53}	—	6.54	2.35
	R181S ^{d,53}	—	5.46	3.73
	H227I ^{d,53}	—	8.30	8.54
	W121A/R118S/H227I ^{d,53}	—	10.2	24.80
	W121I/R181S/H227I ^{d,54}	2.50	3.47	1.15
<i>BtDAPDH</i>	wild-type ^{c,55}	n.d.	—	—
	W129T/D134C/S177A/ F154 V/H235I ^{c,55}	0.7	—	—

^aAll parameters were determined under assay conditions described in the references provided within the table, monitoring the decrease of NADPH by absorbance measurements at 340 nm; "—": activity was not determined; n.d.: no detected activity. ^bSpecific activity. ^cHis-tagged enzyme. ^dNon-tagged enzyme.

within the closed subunit of *UtDAADH* the homologous D75 and R162 are distal (17 Å), as are the loops containing mutated residues Y224F and D94A (8.3 Å; Figure 5a). While these structural highlights suggest that Y224(F) positions at the active site entrance, mutated residue D94, in analogy to its homologue D90 from CgDAADH (PDB: 3DAP), is involved in the fixation of the $-\text{NH}_2$ group of the substrate's D-stereocenter. Docking phenylpyruvate into the closed D94A/Y224F *UtDAADH* revealed that the substrate's phenyl ring is positioned in proximity to sequence position 94; thus,

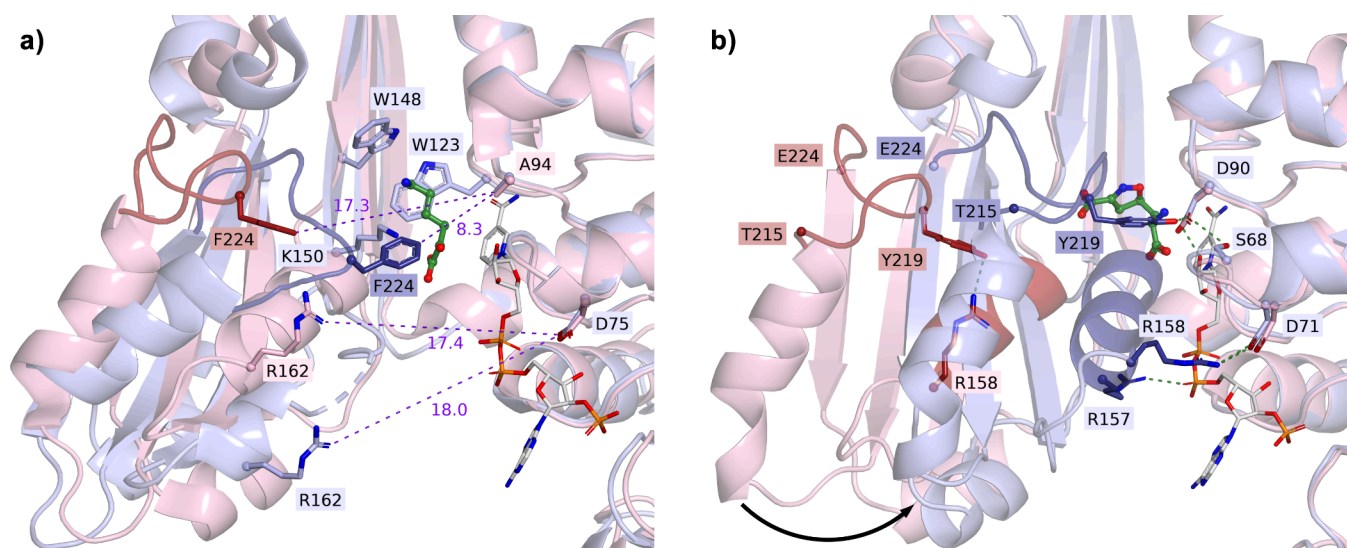


Figure 5. (a) Structural overlay of the open, ligand-free (colored in pink, PDB: 5GZ3) and closed, ligand-bound (colored in blue, PDB: 5GZ6) subunits of the D94A/Y224F *UtiDAADH*; (b) Structural differences between the closed (colored in blue) and open (colored in pink) conformations of the monomeric subunits of *CgDAPDH* (PDB: 3DAP), highlighting loop T215-E224 of *CgDAADH*, incorporating Y219.

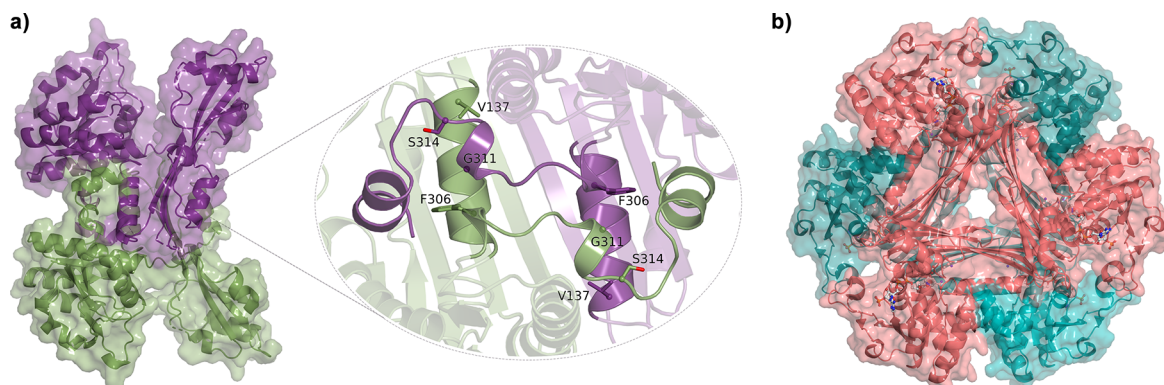


Figure 6. (a) The dimeric fold of type I *UtiDAADH* (PDB: 5GZ6), revealing residues located at the interaction interface between monomers, which have been targeted for mutations within variant V137I/F306W/G311I/S314L;⁴⁵ (b) The hexameric fold of type II *SfiDAADH* (PDB: 3WBF).

mutation D94A increases the active site's hydrophobicity and volume, thereby facilitating the accommodation of aromatic substrates.⁴¹ While the engineered *UtiDAADH* was used to produce several branched chain amino acids, labeled with ¹⁵N and/or ¹³C isotopes,⁴³ its aromatic substrate scope within the reductive amination was not fully explored; only enzyme activities for the production of D-Phe, D-*p*-Phe, and D-*p*-Cl-Phe are being reported.⁴⁴

Its variant V137I/F306W/G311I/S314L was reported to possess an increased optimal temperature of 60 °C in the reductive amination of phenylpyruvate and maintained 93% of its activity at 80 °C, in comparison with the 50 °C optimal temperature and 40% maintained activity shown by *UtiDAADH*.⁴⁵ While the reaction velocity (v_{\max}) was unaffected by the mutations, the substrate affinity increased from a K_M of 1.5 to 1.0 mM (Table 1). While the targeted residues position within the subunit interface of the dimeric *UtiDAADH* (Figure 6a), their mutation into sterically more demanding residues of similar or increased hydrophobicity than the original ones, most probably increased the compactness of the interaction interface and, thus, the stability of the dimer. As a critical note, the reported data do not allow in-depth analysis of the

additional salt-bridges and hydrogen bonds claimed to be formed between the monomers.⁴⁵

To enhance the cost-efficiency of the DAADH-catalyzed reductive aminations, immobilization of *UtiDAADH* on diverse solid supports was tested.^{46,47} By covalent immobilization onto Purolite ECR8415F or co-immobilization with the cofactor regenerating GDH on polyethylenimine-coated agarose beads, *UtiDAADH* maintained its activity over 10 reaction cycles and provided D-phenylalanine with 86% yield in the preparative-scale reductive amination of phenylpyruvate.⁴⁶ By encapsulation-based immobilization, employing a peptide linker and a metal–organic framework support based on zeolitic imidazolate (ZIF-8) and reduced graphene oxide (RGO), the operational stability of *UtiDAADH* was also improved. The DAADH/ZIF-8/RGO maintained 53% of its activity after 10 h of operation at 50 °C, conditions which inactivated the non-immobilized *UtiDAADH*.⁴⁷

Other engineered DAADHs were also developed from DAPDHs of diverse sources by employing homologous mutations to those used for creating *CgDAADH*.³³ The type I DAADH from *C. tetani*⁴⁸ exhibited high activity for the reductive amination of several α -keto acids, however, its

aromatic substrate scope was not explored. Its specific activity of 0.112 U/mg within the reductive amination of phenylpyruvic acid (PPA) is 16-fold lower than of *Ut*DAADH, but 9.3-fold higher than the activity of *Cg*DAADH (Table 1).

The DAPDH from the thermophilic bacterium *S. thermophilum* (*St*DAPDH) represented the first *wild-type* DAPDH with high activity and relaxed substrate specificity in the reductive amination route.⁴⁹ Phylogenetic analysis³⁶ propelled *St*DAPDH as a prototype of type II DAPDHs, characterized by a hexameric quaternary structure (Figure 6b) instead of the dimeric fold of type I DAPDHs (Figure 6a). Insertions/deletions (indels) were identified to be responsible for the divergence within the quaternary structure of the two types of DAPDHs, with both types showing a similar fold of monomers.⁴² *St*DAPDH exhibited a higher thermostability than previous DAPDHs/DAADHs and was shown to possess two substrate entrance tunnels formed at each side of residue M152.⁴² The smaller tunnel allows the entrance of small non-natural substrates such as pyruvate/alanine, while the larger tunnel, common for all DAPDH family members, allows the binding of the bulkier *meso*-DAP (Figure 7).

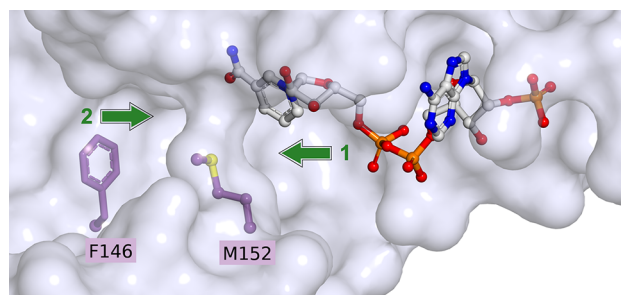


Figure 7. Substrate entrance cavities around residue M152 of *St*DAADH, shown in the NADP⁺-bound *St*DAPDH (PDB: 3WBB). The natural substrate *meso*-DAP follows entrance route 2 (from left to M152), while for small substrates such as pyruvate/alanine transformed atypically by *St*DAPDH, it follows alternative entrance channel 1 (right side of M152).⁴²

The overlay of the open and closed subunits of *St*DAPDH (PDB: 3WBF) and of *Cg*DAPDH (PDB: 1F06) reveals an extra loop (residues 176–191) in *Cg*DAPDH (Figure 8a,b), with most of the catalysis-related residues being conserved, except for F146 and M152, that correspond to W144 and Q150 in *Cg*DAPDH (Figure 9). By loop deletion and alanine-scan mutagenesis, the importance of this loop in maintaining the catalytic activity of *Cg*DAPDH was revealed. An essential salt bridge between R180 and E262 likely stabilizes the loop conformation, which is also influenced by the preceding α -helix starting at L176 and its H-bonding network at the other end of the loop, closed by H193.³⁶ Insertion of this loop within *St*DAPDH significantly decreased its activity, suggesting that the indel loop of type I DAADH is not the key driving force for the divergent evolution of the two DAPDH subtypes.³⁶

Non-active site residue R71 of *St*DAPDH, highly conserved among type II DAPDHs, was found to be a substrate-preference indicator, highlighting the increased preference of this subclass for the amination route.⁵⁰ Positioned in the proximity of the cofactor binding site, R71 is involved in a cation– π interaction with Y205 (Figure 8c). The latter is the homologue of Y224 and Y219 from *Ut*DAPDH and *Cg*DAPDH, respectively, and in the closed subunit of

*St*DAPDH is involved in the H-bonding network with D92, T70, and NADPH, similar to that observed in the closed *Cg*DAADH.^{36,50} Interestingly, R71, positioned within the highly conserved “PTR” sequence of type II DAPDHs (Figure 9), also contributes to the significant difference in catalytic site closure between type I and type II DAADHs (Figure 8c). In type II *St*DAPDH, residue R71, upon domain closure triggered by substrate binding, forms a salt bridge with D203. This salt bridge and the H-bonding between Y205 and D92 provide the movement of α -helix-containing residues 193–203 into the position corresponding to the closed conformation (Figure 8c). Residues Y205 and D92, and most likely also their H-bonding, are conserved in type I DAPDHs (Figure 9). Notably, the mutagenesis of their homologous residues, Y224 and D94 of *Ut*DAADH, provided the improved variants for aromatic substrates.⁴¹ In contrast, residues R71 and D203 are specific to type II DAPDHs (Figures 8c and 9). In type I DAPDHs, the specific salt bridge between D71 and R158 (*Cg*DAADH) repositions a different α -helix (149–158), resulting in the more compact closed conformation characteristic of type I DAPDHs, as seen in the case of *Cg*DAADH (Figure 8b). Notably, the latter helix contains several catalytic residues (e.g., M152 of *St*DAPDH), subjected to previously described protein engineering studies.⁴² In the attempt to transpose the relaxed substrate specificity shown in reductive amination by type II *St*DAPDH into type I DAPDHs, residue A69 of *Cg*DAPDH was replaced by arginine to mimic the R71 of *St*DAPDH. However, the catalytic efficiencies of *Cg*DAPDH within the reductive amination were only slightly increased.⁵⁰ As a critical note, mutation M216D, which provides the ionic counterpart for R69 and enables the complete switch between the catalytic site closure of type I and type II DAPDHs, was not described by the authors.⁵⁰

*St*DAPDH shows 40-fold lower activity for phenylpyruvic acid than for pyruvic acid,⁴⁹ thus, applying the engineering approach used for *Cg*DAADH,³³ the saturation mutagenesis of residues F146, T171, R181, and H227, interacting with the L-center of *meso*-DAP, was performed.⁵¹ Several mutants, including T171S, T171P, and R181F, possessed ~2.5–6.4-fold increased activity, while H227C and H227V showed the highest at ~15- and ~35-fold activity improvements over *wild-type* *St*DAPDH (Table 1).⁵¹ Computational results suggested that within the active site of variant H227V, the substrate is pulled closer to NADPH, with its phenyl ring interacting only with T171, whereas in *wild-type* *St*DAPDH it forms interactions with three residues F146, H227, and S151 (Figure 10). At 0.1 mmol-scale, variant H227V catalyzed the reductive amination of phenylpyruvic acid to D-phenylalanine, with 97% conversion and 99% enantiomeric excess.⁵¹ Variant H227V was also employed in a cascade reaction with L-amino acid deaminase from *Proteus mirabilis* (*Pma*LAAD) for the efficient stereoinversion of L-Phe analogues to their D-counterparts (see Section 5.3).

To tailor *St*DAPDH toward the synthesis of D-homophenylalanine, D-phenylglycine, and D-tryptophan, additional five residues, D92, W121, M152, H154, and N253, were subjected to saturation mutagenesis.⁵² Only libraries of W121, T171, and H227 generated improved variants, while randomization of residue D92 or the D92A variant (analogue of D94A *Ut*DAADH of enhanced activity toward phenylpyruvic acid⁴¹) did not provide superior activity. The best performing W121L/H227I mutant showed 34-fold and 70-fold improved enzyme activity toward 2-oxo-4-phenylbutyric acid and

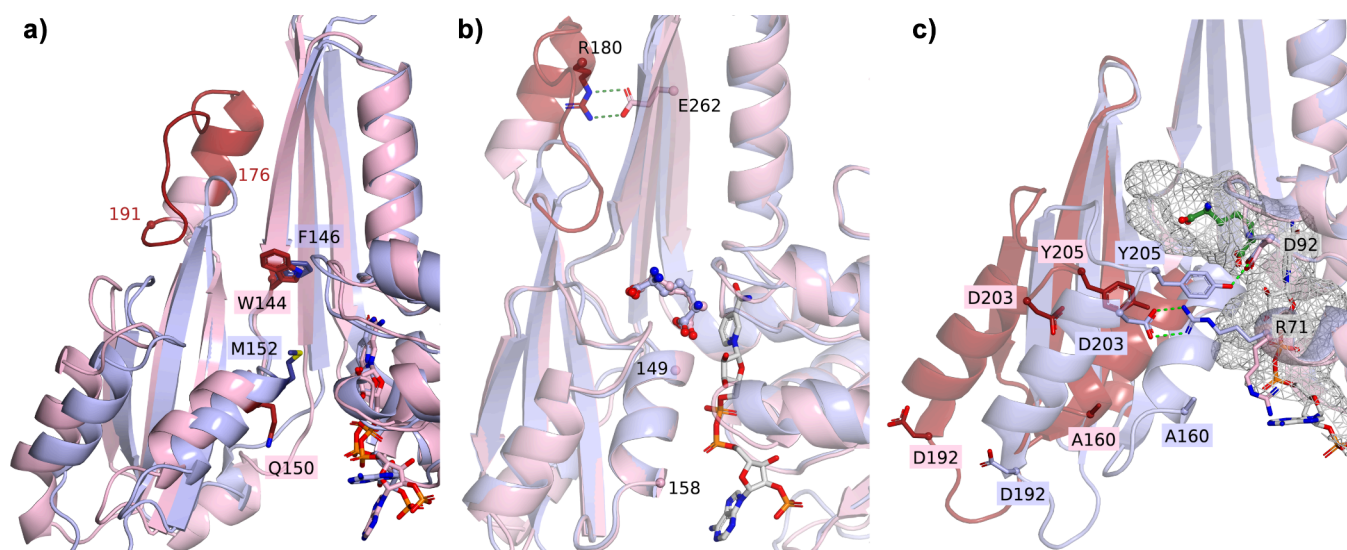


Figure 8. (a) The overlay of open conformations of type II *StDAADH* (blue, PDB: 3WBB) and type I *CgDAADH/CgDAPDH* (pink, PDB: 1F06, chain A); (b) The closed monomer of *StDAADH* (blue, PDB: 3WBF) overlaid with the closed conformation of *CgDAADH* (pink, PDB: 1F06, chain B). Residues 176–191 are highlighted in dark red in (a) and (b); (c) Overlay of the open (pink, PDB: 3WBB) and the closed, ligand-bound (DAP, green) structures of *StDAPDH* (blue, PDB: 3WBF) showing the salt-bridge between R71 and D203, which provides the conformational movements of the corresponding α -helices, specific to the closure of type II DAADHs.

	67	71	90	119	124	144	149	158	167	169	176		191	193	195	216	219	244	262	270
<i>CgDAPDH</i>	GSATD	D	WDPGMF	W	SGHSDALRR	QYT	LEKARRGEAGDLTGKQ	HKR	M	Y	H	E	N							
<i>UdDAPDH</i>	GSATD	D	WDPGLF	W	SGHSDAIRR	QYT	VNRVRSNGENPELTRE	HAR	M	Y	H	E	N							
<i>CdDAPDH</i>	GSATD	D	WDPGLF	W	SGHSDAIRR	QYT	LDKARSGEQCDFTTRE	HER	M	Y	H	E	N							
<i>LdDAPDH</i>	GSATD	D	WDPGLF	W	SGHSDAVRR	QYT	VDRVRNGENPELTRE	HAR	M	Y	H	E	N							
<i>TdDAPDH</i>	PTRSV	D	WDPGTD	F	SMGHSVALKA	SMT	-	HRR	D	Y	H	S	N							
<i>NmDAPDH</i>	PTRTI	D	WDPGTD	F	SMGHSVAVKA	SLT	-	HRR	D	Y	H	T	N							
<i>PvDAPDH</i>	PTRAII	D	WDPGSD	F	SMGHSVAAKA	SMT	-	HRR	D	Y	H	E	N							
<i>BdDAPDH</i>	PTRET	D	WDPGTD	F	SMGHSVAVKA	SLT	-	HRR	D	Y	H	T	N							
<i>StDAPDH</i>	PTRSV	D	WDPGTD	F	SMGHSVAVKA	SMT	-	HKR	D	Y	H	R	N							
	69	73	92	121	126	146	151	160	169	171		179	181	203	205	227	246	253		

Figure 9. Sequence alignment of type I and type II DAPDHs employed within the synthesis of D-phenylalanines. The conserved amino acids in type I DAPDHs are in blue, and those conserved in type II DAPDHs are in green, while purple represents those conserved in both type I and type II DAPDH. Residues marked in red are part of the insert loop of type I DAPDHs, while those highlighted in gray were subjected to the protein engineering efforts highlighted in this study.

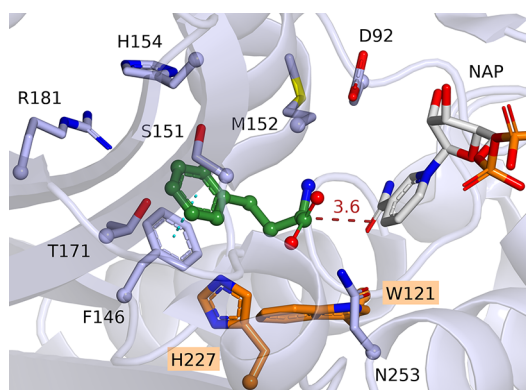


Figure 10. Phenylpyruvate docked within *wt-StDAADH* (PDB: 3WBB), highlighting the relative positioning of W121 and H227 to the aromatic ring of the substrate. The docking results have been reproduced with permission using Autodock Vina by following the reported data.⁵²

phenylpyruvic acid, respectively, while also catalyzing the reductive amination of both phenylglyoxylic acid and indole-3-pyruvic acid (Figure 11). Enzyme kinetics revealed an

increased catalytic velocity for the mutants, with the mutations having less impact on the K_M values. Docking studies suggested a substrate binding pocket reshaped by mutations W121L and H227I, thereby altering substrate orientation in comparison to the *wild-type* form (Figure 10).⁵² The substrate's aromatic ring positions between L121 and I227, with a reduced distance between the α -hydrogen of D-homophenylalanine and the C4 of nicotinamide mononucleotide, suggest a facilitated hydride transfer from/to the cofactor within the mutant variant. Employing this engineered variant, the preparative, 1 mmol-scale reaction yielded D-phenylalanine in excellent 85% yield, with a high optical purity of $ee > 99\%$.

The same tension release approach was employed for engineering type II DAPDH from *Proteus vulgaris*. *PvDAPDH* shares a high, 63.6% sequence identity with *StDAPDH*, thus, saturation mutagenesis was implemented at five residues from which four positions (W121, F146, T171, H227) were identical with those studied in the case of *StDAPDH*.⁵³ The saturation mutagenesis at the additional catalytic residue R181 provided variant W121A/R181S/H227L, with an 85-fold and 4-fold increase in catalytic efficiency (k_{cat}) within the reductive amination of phenylpyruvate compared to *wt-PvDAPDH* and W121L/H227I *StDAPDH*, respectively (Table 1).⁵³ The

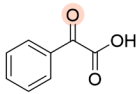
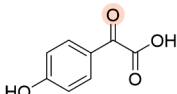
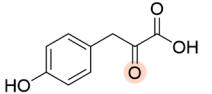
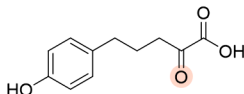
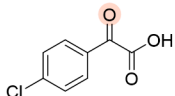
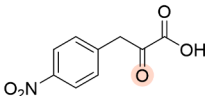
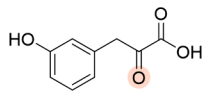
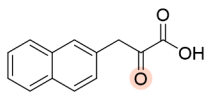
Enzyme		S.A. (U/mg)	K_M (mM)	k_{cat} (s ⁻¹)		S.A. (U/mg)	K_M (mM)	k_{cat} (s ⁻¹)		S.A. (U/mg)	K_M (mM)	k_{cat} (s ⁻¹)		S.A. (U/mg)	K_M (mM)	k_{cat} (s ⁻¹)
wild-type PvDAPDH ⁵⁴	0.100	7.34	0.61	n.d.	0.200	12.41	0.46	0.020	1.85	0.06						
W121I/R181S/H227I ⁵⁴	0.500	1.70	0.41	0.100	2.300	3.02	1.31	2.500	2.41	1.27						
wild-type BtDAPDH ⁵⁵	0.006	4.96	0.01	0.140	n.d.			0.300								
W129T/D134C/F154V/S177A/H235I ⁵⁵	1.650			0.340	0.120			3.660								
wild-type StDAPDH ⁵²	n.d.							0.380								
W121L/H227I ⁵²	0.240							6.890								
		S.A. (U/mg)				S.A. (U/mg)				S.A. (U/mg)				S.A. (U/mg)		
wild-type PvDAPDH ⁵⁴	n.d.				0.300			0.200					n.d.			
W121I/R181S/H227I ⁵⁴	0.800				2.100			2.700					2.000			

Figure 11. Tested aromatic substrate scope of type II StDAPDH, PvDAPDH, and BtDAPDH and their engineered variants.

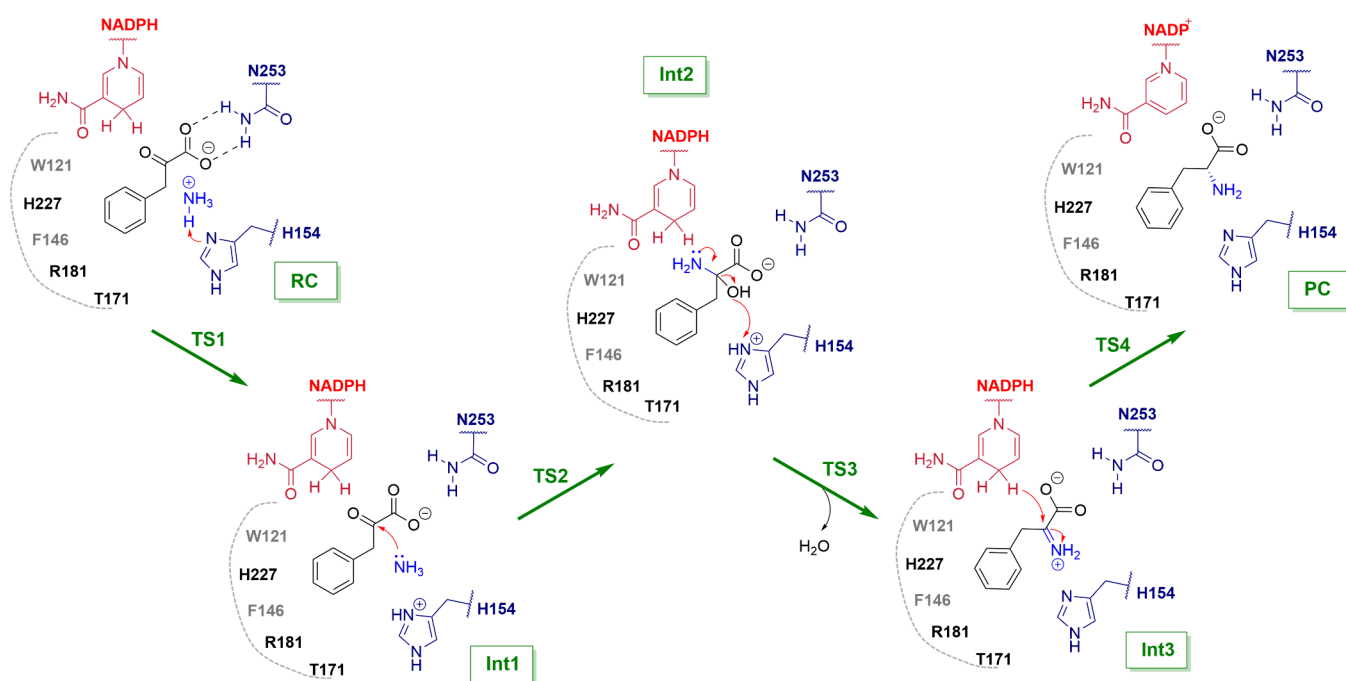


Figure 12. Four-step reaction mechanism for the PvDAPDH-catalyzed reductive amination of the phenylpyruvate reactant (RC) into the D-Phe product (PC), involving three reaction intermediates (Int1–Int3). The residues (in gray) from the hydrophobic substrate binding region are positioned below the plane of the substrate's aromatic moiety, while bolded residues are in or above this plane. Reproduced with permission from ref 54. Copyright 2024 American Chemical Society.

engineered PvDAPDH was used in combination with LAAD (see Section 5.3) within a 3 L-scale one-pot conversion of L-Phe to D-Phe with a 57.8 g·L⁻¹ titer, 95.7% yield, and 99% ee.⁵³

Using quantum mechanical (QM) calculations, a four-step molecular mechanism for the PvDAPDH-catalyzed reductive amination of phenylpyruvate has been proposed,⁵⁴ in which after cofactor and substrate binding, residue H154 acts as a general base to deprotonate NH₄⁺, which attacks the carbonyl group of intermediate 2 (Figure 12). Residues W121, F146, T171, R181, and H227, in analogy to the role of homologous residues in StDAPDH, form the narrow L-pocket, which restricts the rotation of the phenylpyruvate. Saturation mutagenesis of these five residues and the subsequent

combination of the beneficial mutations provided the triple mutant W121I/R181S/H227L PvDAPDH, with a catalytic constant of 1.15 s⁻¹ within the reductive amination of PPA,⁵⁴ 21.5-fold lower than the previously identified W121A/R181S/H227L variant.⁵³ In both engineered PvDAPDHs similar mutations of the same residues were identified within the best performing variants of the SM-libraries, suggesting a limited variety of beneficial mutations. The specific activity and enzyme kinetics of variant W121A/R181S/H227L were assessed for several aromatic keto acids (Figure 11), being also employed as biocatalyst in a three-component cascade for the synthesis of aromatic D-amino acids (see Section 5.3).⁵⁴

The structure-guided engineering of another database-identified type II DAPDH from *Bacillus thermozeamaize* (*BtDAPDH*), sharing 65% sequence identity with *StDAPDH*, targeted 43 residues within the 8 Å surrounding the docked benzoylformic acid substrate for individual NNK-saturation mutagenesis.⁵⁵ Randomization of the first layer, built from catalytic site residues within a 0–4 Å distance to the substrate, provided the best performing variant W129T/F154V/H235I. All three residues are located at the narrow L-pocket of the enzyme and are homologues of the previously randomized residues of *StDAPDH*⁵² and *PvDAPDH*⁵⁴ (Figure 9). The engineering carried out at residues from the second and third layers, with 4–6 and 6–8 Å distances to the substrate, revealed beneficial mutations D134C and S177A. When combined with the first-layer mutations, the resulting variant W129T/D134C/F154V/S177A/H235I exhibited the highest activity in the reduction of benzoylformate. While the *wild-type* enzyme showed no activity toward aromatic keto acids, the engineered variant showed high, 0.7 and 0.12 U/mg, specific activity for phenylpyruvate and *p*-OH-phenylpyruvate (Figure 11).⁵⁵ The synthetic applicability of the engineered *BtDAADH* was demonstrated in the 100 mL-scale reductive amination of a 100 mM phenylpyruvate solution producing 1.42 g D-phenylalanine with 86% yield (Table 1).⁵⁵ Mutations W129T, F154V, and H235I, similar to those of *StDAPDH* and *PvDAPDH*, increased the substrate affinity by a more spacious hydrophobic binding pocket. Further, the structure of the engineered *BtDAADH* (PDB:8ZMX) docked with benzoylformic acid revealed that D134, by interacting with D130, highly influences the positioning of W129, with the latter contributing to the steric hindrance within the hydrophobic, narrow L-pocket of the wild-type enzyme. By mutations of both residues, the steric hindrance is eliminated and the electrostatic interaction between D134 and D130 is replaced by H-bonding between C134 and T129, maintaining the structural stability of the catalytic pocket. Residue S177 H-bonds with S159, which is involved in the fixation by H-bonding of the substrate's carboxylate. Mutation S177A strengthens the H-bonding to S159 and alters the conformation of the loop, including S177, while also disrupting the H-bonding between M160 and the substrate's carbonyl group, thus facilitating alternative substrate conformations.⁵⁵

Other engineering approaches targeted the cofactor binding region of *StDAPDH*, resulting in variant K159R, which is able to operate with the less expensive NADH, albeit showing a 6-fold lower k_{cat} than with the natural cofactor, NADPH.⁵⁶ Sequence-based identification of novel thermophilic meso-DAPDHs revealed DAPDH from *N. massiliense*⁵⁷ and *T. lipolytica*⁵⁸ is capable of operating with both NADP⁺ and NAD⁺; however, the reductive amination in the presence of NADH did not occur.

3. ASYMMETRIC SYNTHESIS BY AMINOTRANSFERASES

D-Amino acid transaminases (DAATs) have been identified in several bacterial species as being involved in the production of D-amino acids that are necessary for the biosynthesis of peptidoglycans and secondary metabolites.^{59–63} Their common mechanism involves the shuttling of the pyridoxal-5-phosphate (PLP) cofactor between its pyridoxal and pyridoxamine forms, coupled with the reversible transfer of the amino group between the amino acid–keto acid substrate pair (Figure 13). Since aminotransferases (ATs) typically exhibit

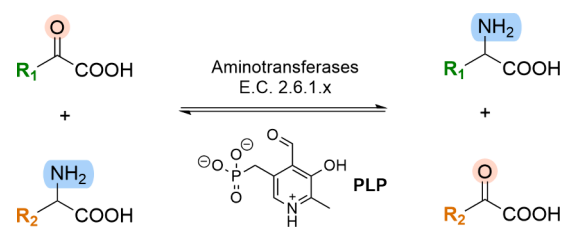


Figure 13. Reversible amino group transfer reaction catalyzed by ATs (EC 2.6.1.x).

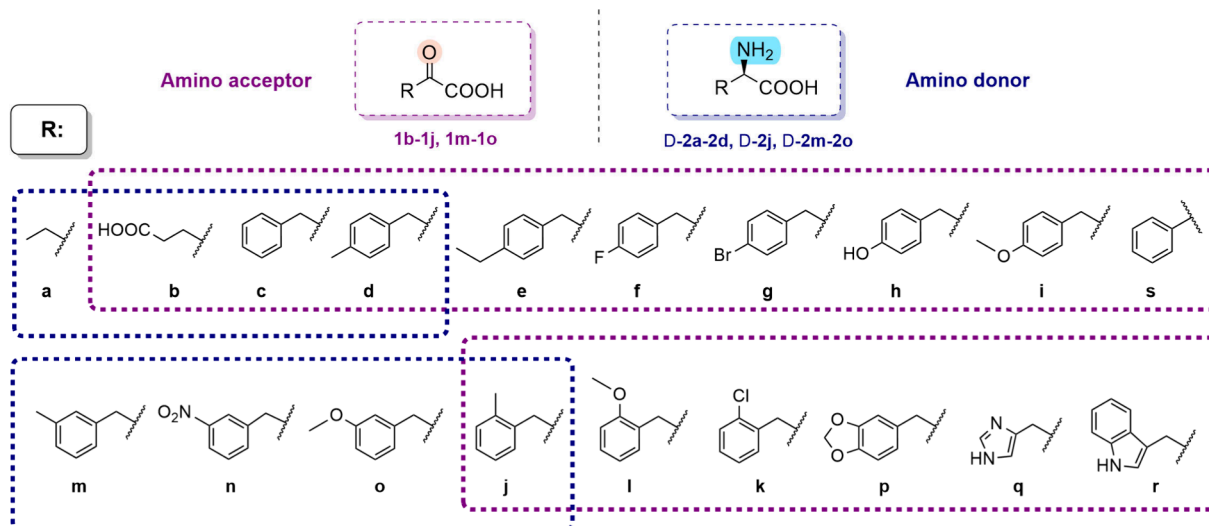
an equilibrium constant close to unity, several strategies have been employed to drive the reaction to completion. These include amino donor recycling through auxiliary enzymatic reactions^{64,65} or by enzymatic decomposition of the keto acid byproduct.⁶⁶

Among the first explored D-amino acid transaminases, DAAT from *Bacillus sphaericus* presented broad substrate specificity for both amino donor and amino acceptor substrates. Albeit, when using phenylpyruvate and D-alanine as reaction partners, low relative activity was obtained (Table 2).⁶³ DAATs from *Staphylococcus hemolyticus*,⁶⁷ *Bacillus licheniformis*,⁶⁸ and *Bacillus sphaericus*⁶⁹ overexpressed in *E. coli* were also employed for the production of several D-amino acids, including D-Phe.⁷⁰ The database-identified DAAT from *Lactobacillus salivarius* substantially differed from the other DAATs by exhibiting a broad amino acceptor specificity for keto acids (Table 2), including bulky aromatic compounds such as indole-3-pyruvate and 4-hydroxyphenyl-pyruvate.⁷¹ Despite their broad substrate specificity, the industrial applicability of the DAAT-mediated process has been limited by the position of the reaction equilibrium, with K_{eq} being close to 1. To shift the equilibrium to the desired direction by a process developed by the Monsanto Co.,⁷⁰ the DAAT reaction was integrated into a biosynthetic cascade (detailed in Section 5.4) within an engineered *E. coli*. The engineered strain, besides expressing *BsDAAT*, had the *tyrB*, *aspC*, and *ilvE* aminotransferase genes disrupted to enhance the supply of phenylpyruvate for DAAT-mediated D-Phe production. The biosynthetic cascade, with an external addition of the D,L-Ala amino donor, produced enantiopure D-Phe at a titer of 4.15 g/L. By feeding the fermentation with L-Phe as phenylpyruvate precursor, the titer significantly increased to 13.7 g/L, however, the enantiomeric excess of D-Phe decreased to 88%.

In another approach, DAATs have been coupled with ω -transaminase (TA) of (R)-selectivity, which enables the regeneration of the D-amino acid amino donor of the DAAT reaction (Figure 14).⁷² Using *BsDAAT* and ARmutTA (Rd11-TA), engineered for bulky ketones,⁷³ along with D-Ala or isopropylamine as the amino donor, the procedure achieved complete conversion of phenylpyruvate into the enantiopure D-Phe in a 3 h reaction time (Table 2).⁷²

The comparison of the activity toward phenylpyruvate of recombinant DAATs which is originally from *Bacillus* strains, *B. subtilis* (*BsDAAT*), *B. licheniformis* (*BIDAAT*), and *B. amyloliquefaciens* (*BaDAAT*), revealed *BIDAAT* with the highest specific activity (Table 2).^{71,74} Despite its lower activity, due to its higher expression levels, *BsDAAT* was included within the D-Phe synthetic operon constructed in *E. coli*.⁷⁴ This engineered *E. coli*, besides incorporating the gene deletions employed by the Monsanto Co.,⁷⁰ also included the disruption of the D-amino acid dehydrogenase (*DAADH*) encoding gene, which alleviated the cellular deamination of the

Table 2. Summary Table with Specific Activities (SA), Kinetic Parameters, Conversion (*c*), and Enantiomeric Excess (*ee*) Values for the DAAT-Mediated Transaminations of Amino Acceptor α -Keto Acids 1b–1j and 1m–1o, using D-Amino Acids D-2a–2d, D-2j, and D-2m–2o as the Amino Donors^a



DAAT original strain	enzyme	amino donor	amino acceptor	product	SA ^b (U/mg)	<i>c</i> (%)	<i>ee</i> (%)	<i>K_M</i> (mM)	<i>k_{cat}</i> (s ⁻¹)	<i>k_{cat}/K_M</i> (s ⁻¹ mM ⁻¹)
<i>L. salvarius</i> ⁷¹	DAAT	D-2a	1c	D-2c	10.94	-	-	-	-	-
			1h	D-2h	24.34	-	-	-	-	-
			1r	D-2r	48.92	-	-	-	-	-
<i>G. toebii</i> SK1 ⁷¹	DAAT	D-2a	1c	D-2c	0.48	-	-	-	-	-
<i>B. subtilis</i> ⁷¹	DAAT	D-2a	1c	D-2c	0.24	-	-	2.47	0.22	0.890
<i>B. licheniformis</i> ⁷⁴	DAAT	D-2a	1c	D-2c	0.03	-	-	3.09	3.63	1.175
<i>B. amylolichifaciens</i> ⁷⁴	D-AAT	D-2a	1c	D-2c	0.46	-	-	2.05	2.23	1.088
<i>B. sphaericus</i>	DAAT ⁷¹	D-2a	1c	D-2c	0.55	-	-	-	-	-
	DAAT/Ar _{mut} TA ⁷²	D-2a, IPA	1c	D-2c	-	99	>99	-	-	-
			1s	D-2s	-	97	>99	-	-	-
YM-1 <i>B. sp</i>	DAAT ⁷¹	D-2a	1c	D-2c	2.89	-	-	-	-	-
	DAAT-T242G ⁶⁵	D-2b	1c	D-2c	-	>99	95 (99) ^c	-	-	-
			1f	D-2f	-	>99	92 (>99) ^c	-	-	-
			1k	D-2k	-	>99	92 (>99) ^c	-	-	-
			1g	D-2g	-	98	80 (98) ^c	-	-	-
			1j	D-2j	-	98	93 (98) ^c	-	-	-
			1d	D-2d	-	98	93 (98) ^c	-	-	-
			1e	D-2e	-	>99	97 (>99) ^c	-	-	-
			1l	D-2l	-	97	99 (>99) ^c	-	-	-
			1i	D-2i	-	>99	99 (>99) ^c	-	-	-
			1p	D-2p	-	98	96 (>99) ^c	-	-	-
		D-2c	1b	1c	1.21	-	-	4.50	1.80	0.400
		D-2j	1j	1j	0.32	-	-	16.00	0.74	0.450
		D-2m	1m	1m	0.51	-	-	3.70	2.60	0.703
		D-2o	1o	1o	-	-	-	6.00	2.20	0.367
		D-2n	1n	1n	-	-	-	5.30	0.44	0.830
		D-2d	1d	1d	2.12	-	-	5.00	2.20	0.449
	DAAT-S240G ⁶⁵	D-2b	1c	D-2c	-	-	-	15.00	0.58	0.039
	DAAT ⁶⁶	D-2b	1c	D-2c	-	-	-	6.70	0.09	0.014
	DAAT-V33G ⁶⁶	D-2b	1c	D-2c	-	-	-	2.10	0.10	0.048

^aAll parameters were determined under the assay conditions from the corresponding references. ^bSA: specific activity; 1 unit (U) defined as the amount of enzyme catalyzing the formation of 1 μ mol product per min; in the case of DAATs from ref 69, the specific activities were calculated by the authors of this Review based on the reported relative activity values and experimental data. ^cValues obtained with the whole-cell biocatalyst; values in parentheses were obtained with a purified enzyme.

produced D-Phe. In a 15 L jar fermentation process, the engineered strain yielded D-Phe with a titer of 1.72–3.86 g/L; however, despite reporting the formation of L-Phe, data related to the product's enantiomeric excess was not included.⁷⁴

Through rational design, the specific activity for D-phenylalanine is shown by DAAT from *Bacillus sp.* YM-1 was increased by 2 orders of magnitude,⁶⁵ approaching its natural activity for D-alanine.⁷⁵ Targeting residues V33, S240, and

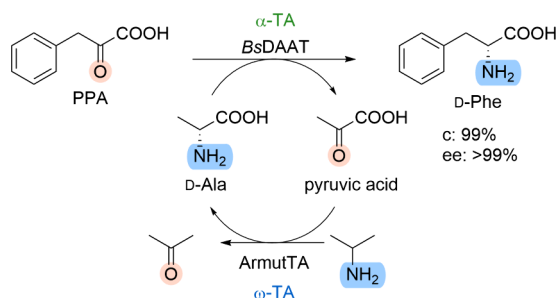


Figure 14. Coupled enzymatic reactions for the reductive amination of PPA with D-Ala and isopropylamine as amino-donors and using *Bacillus sphaericus* DAAT as the α -aminotransferase and ARmutTA as the ω -transaminase of (R)-selectivity.⁷²

T242, responsible for the accommodation of the aromatic ring of D-Phe, and mutation V33G led to a 3-fold increase in the catalytic efficiency ($k_{\text{cat}}/K_M = 0.048 \text{ s}^{-1}\cdot\text{mM}^{-1}$), while the T242G variant showed the highest, 615-fold increase in activity toward D-Phe ($\sim 1.21 \text{ U/mg}$), reaching the activity of the wild-type DAATs for D-alanine ($\sim 1.10 \text{ U/mg}$) (Table 2).⁷⁶ Residue V33 is located within a β -strand, whereas S240 and T242 are part of the 204–243 loop within the substrate's side-chain binding pocket (Figure 15). Substituting these residues with the less flexible and smaller glycine contributes to tailoring the side-chain binding pocket toward bulkier substrates.⁶⁵

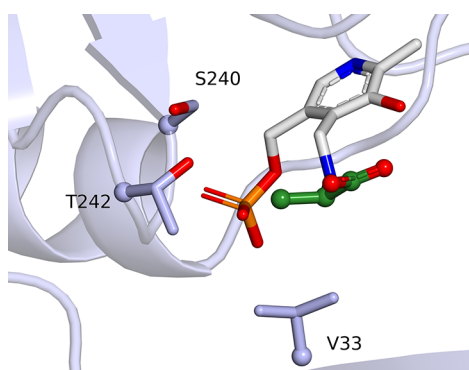


Figure 15. Catalytic site of YM-1 BsDAAT (PDB: 3DAA)⁷⁷ with the D-alanine amino donor (green) bound to the pyridoxal phosphate (PLP) cofactor (gray) within the substrate binding pocket, including residues V33, S240, and T242.

The activity of the engineered T242G YM-1 BsDAAT toward various monosubstituted phenylalanines was tested, obtaining several D-phenylalanines with high conversions ($\geq 97\%$) over a 12 h reaction time (Table 2).⁶⁵ Further, DAAT-T242G was used with LAAD from *Proteus mirabilis* in the form of a whole-cell biocatalyst within stereoinversion and deracemization cascades, producing D-phenylalanines from their L-enantiomeric counterparts⁶⁵ (see Section 5.4).

4. ASYMMETRIC HYDROAMINATION BY PHENYLALANINE AMMONIA-LYASES

Phenylalanine ammonia-lyases (PALs, EC 4.3.1.24/25) are among the most studied biocatalysts to produce L-phenylalanines.¹ While PALs within their natural reaction catalyze the dehydroamination of L-Phe, in synthetic applications, starting from racemic phenylalanines, the nonreactive D-amino acids can be obtained through a kinetic resolution-type process that

is limited by a theoretical yield of 50%.^{78–80} In the presence of high ammonia concentrations (4–6 M), PALs catalyze the reverse, asymmetric hydroamination reaction of cinnamic acids, yielding L-amino acids. The asymmetric hydroamination is of high synthetic interest, with PAL-based industrial processes already established, such as the multiton-scale production of (S)-2,3-dihydro-1H-indole-2-carboxylic acid by DSM⁸¹ and the synthesis of (3S)-5-(benzyloxy)-2-(diphenylacetyl)-6-methoxy-1,2,3,4-tetrahydroisoquinoline-3-carboxylate (Olodanrigan or EMA 401) by Novartis.⁸² The substrate scope of PALs has been extended by protein engineering,^{79,83–89} while the reversal of their natural L-enantioselectivity was also attempted, aimed to create D-selective PALs that are capable of producing D-phenylalanines by the hydroamination route. In this case, saturation mutagenesis, targeting 48 catalytic site-related residues of PAL from *Anabeana variabilis* (AvPAL), revealed variants H359Y and H359K with 3.5-fold and 3.3-fold increased activity within the formation of D-p-NO₂-Phe, respectively (Figure 16).⁹⁰ In a similar study, the AvPAL

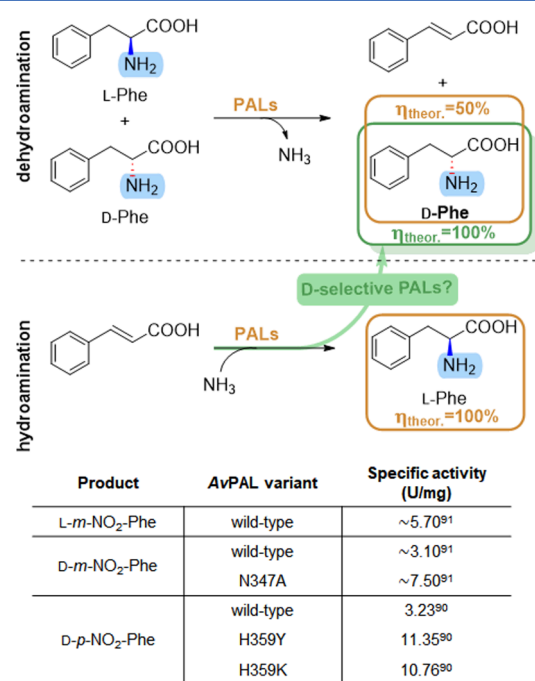


Figure 16. PAL-mediated dehydroamination and hydroamination routes and the activity values of engineered AvPALs in the hydroamination reactions, producing D-m-NO₂- and D-p-NO₂-phenylalanines.

variant N347A showed a 2.3-fold increase in activity within the hydroamination to D-m-NO₂-Phe when compared to the wild-type enzyme.⁹¹ Importantly, the increased D-selectivity mostly occurred in the case of substrates with electron-withdrawing ring substituents for which wild-type PALs also yield phenylalanines of decreased enantiopurity, with the D-enantiomers being observed as the minor product and the L-Phe as the main product.⁹⁰

For the production of D-Phe, alternative reaction mechanisms have been proposed.⁹² The common mechanism of PALs (Figure 17a) requires the highly electrophilic, post-translationally formed 4-methylene-imidazol-5-one (MIO) prosthetic group. In the hydroamination reaction, under high ammonia concentration, the MIO group is aminated, forming

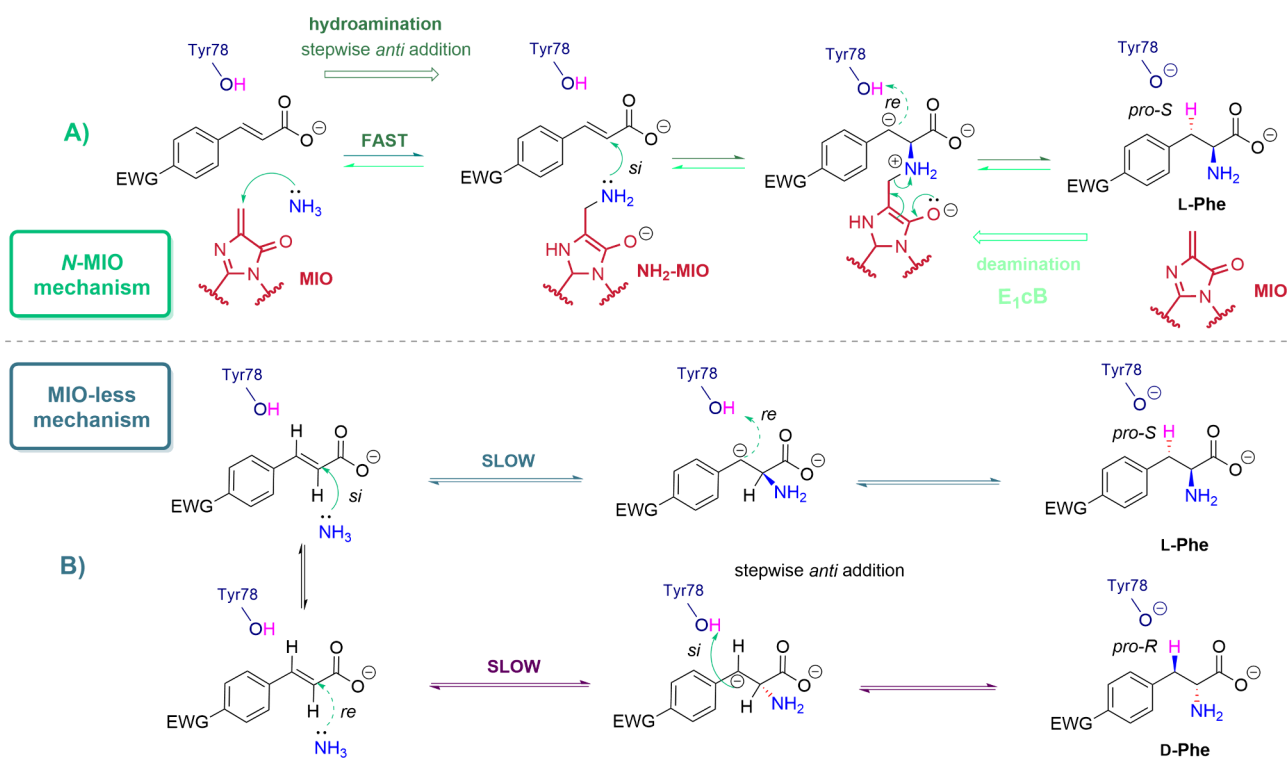


Figure 17. (a) The mechanism of PALs within the L-selective hydroamination reaction, involving the formation and electrophilic attack of the NH_2 -MIO complex and within the reverse deamination of L-Phe; (b) The MIO-less mechanism providing both L- and D-phenylalanines, occurring within the hydroamination of cinnamic acids with electron-withdrawing aromatic substituents. Reproduced with permission from ref 92. Copyright 2014 John Wiley and Sons.

the nucleophilic NH_2 -MIO intermediate, which attacks the α,β -double bond of the cinnamic acid substrate in a regio- and enantioselective manner.^{93,94} Subsequently, the protonation at the β -position is facilitated by a catalytically essential, highly conserved tyrosine, Tyr78, in the case of AvPAL. For the low enantioselectivities registered for substrates with strong electron-withdrawing ring substituents (nitro-, trifluoromethyl, bromo- and chloro-), the occurrence of a non-stereoselective MIO-independent reaction mechanism, capable of producing both L- and D-phenylalanines, has been proposed.⁹² Kinetic data obtained for *wild-type* AvPAL and H359Y, H359K variants, along with isotopic-labeling studies and molecular modeling, suggest that Tyr78 is responsible for the abstraction of the *pro-S* or *pro-R* benzylic protons in the E_1cB mechanism-driven deamination of L-Phe or D-Phe, correspondingly (Figure 17b). The electron-withdrawing effect of the ring-substituent might stabilize the resulting intermediate carbanion, slowing its reprotonation in the deamination route and in this way facilitate the slower, non-stereoselective MIO-independent hydroamination step. For the L-selective process, the *si*-face of the C_α points toward the amino-donor (ammonia or the NH_2 -MIO adduct in the MIO-mechanism) and Y78 points toward the *re*-face of the C_β . However, to produce D-Phe, the binding orientation of the cinnamic acid should be altered, with the *re*-face of C_α pointing toward the amino-donor and Tyr78 pointing toward the *si*-face of C_β (Figure 17b).⁹² The two different productive binding modes of the cinnamic acid are also supported by the mechanism of MIO-dependent phenylalanine aminomutases (PAMs) of different stereoselectivities, which involves the *trans*-cinnamic acid intermediate in two binding conformations, allowing the

exchange of the positions of the *si*- and *re*-faces of C_α and C_β relative to the MIO group.^{95–97}

The mutated residues H359 and N347 of AvPAL are highly conserved among PALs, while positioned within the polar substrate binding region, they participate in the extensive H-bond network, which also includes the essential R317, responsible for substrate fixation, through salt-bridging with the substrate's carboxylate (Figure 18). While this H-bond network controls the different binding orientations of the substrate, its perturbation by mutations of H359 and N347 might facilitate the alternative active site orientations of cinnamic acid, required for D-selectivity.^{90,91}

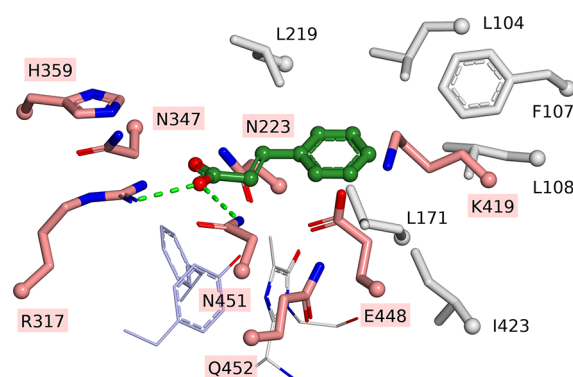


Figure 18. Orientation and fixation of the co-crystallized cinnamic acid within the catalytic site of the AvPAL variant (PDB: SLTM),⁹⁸ highlighting the residues from the polar binding region, including H359, N347, and R317.

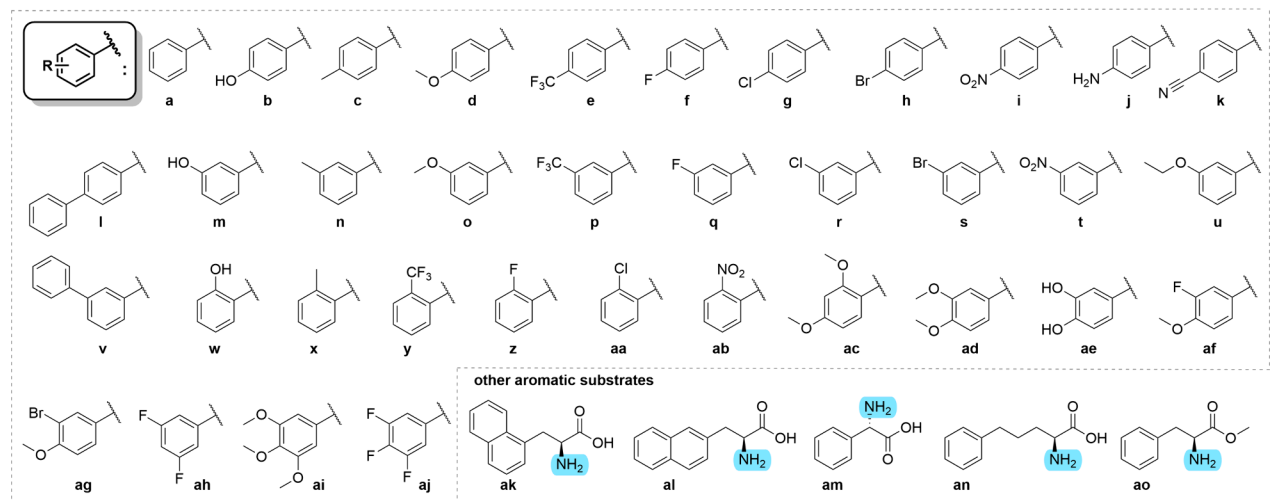


Figure 19. Enzyme cascades producing D-phenylalanines D-1a–1ao, which involve LAAD/LAAO-mediated oxidation coupled with enzymatic asymmetric synthesis routes based on DAADH, DAAT, and PAL-mediated reactions, including the appropriate cofactor regeneration systems.

Despite the developed PAL variants showing increased specific activity toward the formation of the D-*p*-NO₂-Phe during kinetic measurements, in the hydroamination reactions, the final position of the equilibrium between the production of L- and D-enantiomers was maintained, without the useful enrichment of the produced D-enantiomer.⁹⁰ Nonetheless, when variant H359Y was combined with the L-amino acid deaminase (LAAD) from *Proteus mirabilis* (see Section 5.4), the efficient synthesis of D-phenylalanines bearing electron-withdrawing ring substituents was achieved.

5. ENZYME CASCADES INVOLVING ASYMMETRIC SYNTHESIS

The relatively low availability of phenylpyruvates, the starting materials of asymmetric reductive aminations, caused by their tedious synthesis and/or stability issues,^{99,100} has been the driving force for the development of enzyme cascades that focus on their *in situ* generation and simultaneous transformation. In contrast, racemic or L-phenylalanines are more accessible through chemical synthesis or fermentation processes¹⁰¹ and can be readily oxidized to their imino acid or keto acid derivatives, which by simultaneous D-selective or

Table 3. Kinetic Parameters of the *Pmir*LAAD or *Pma*LAAD-Catalyzed Deamination of Different Aromatic Substrates (for Substrate Numbering, see Figure 19), Determined under the Reported Assay Conditions (See References Provided within the Table)

	variant	substrate	K_M (mM)	v_{max} (U/mg)	k_{cat} (s ⁻¹)	k_{cat}/K_M (mM ⁻¹ ·s ⁻¹)
<i>Pmir</i> LAAD	wild-type ¹⁰⁶	L-1a (L-Phe)	21.5	—	1.12	0.050
	wild-type ¹⁰⁶		26.4	—	1.40	0.055
	P93S/P186A/F184L ¹⁰⁶		15.8	—	3.75	0.230
	P93S/P186A/M394V ¹⁰⁶		16.2	—	2.85	0.170
	P93S/P186A/M394V/F184S ¹⁰⁶		12.3	—	4.50	0.360
	T105A/D144A/E145A/E430A/S412A/E417A ¹¹⁵		32.6	—	2.90	0.088
	E145A/L341A ¹¹²		75.6	—	2.04	0.002
	D165 K/F263M/L336 M ¹¹³		22.0	2.63	2.25	0.102
<i>Pma</i> LAAD	wild-type	L-1a (L-Phe) ¹¹⁸	1.60	3.00	—	—
		L-1a (L-Phe) ¹²⁰	1.60	—	2.66	1.66
		(±)-1an ¹¹⁸	2.54	1.51	—	—
		L-1i ¹¹⁸	0.36	2.66	—	—
		L-1ad ¹¹⁸	5.37	1.36	—	—
		(±)-1ak ¹¹⁸	0.79	1.18	—	—
		L-1ak ¹¹⁹	0.79	—	1.05	1.30
		L-1a (L-Phe)	3.76	—	1.36	0.36
	F318A ¹¹⁹	L-1ak	0.24	—	1.02	4.30
		L-1a (L-Phe)	7.38	—	1.41	0.19
	V412A/V438P ¹¹⁹	L-1ak	0.52	—	1.55	3.00
		L-1a (L-Phe)	5.95	—	0.63	0.11
	F318A/V412A/V438P ¹¹⁹	L-1a (L-Phe)	5.95	—	0.63	0.11
		L-1ak	0.17	—	1.57	9.20

non-selective reduction coupled with L-selective oxidation can provide the D-phenylalanines (Figure 19).¹⁰² In these deracemization or stereoinversion processes, using as starting material the racemic or L-Phe, respectively, the required oxidation step can be performed by two FAD-dependent enzymes, L-amino acid deaminases (LAADs) and L-amino acid oxidases (LAOs) (Figure 19). Notably, the engineering of LAADs and LAOs was essential, both for their efficient recombinant expression and to increase their substrate tolerance toward various phenylalanines, as presented in Sections 5.1 and 5.2. While LAADs have been used predominantly in the form of whole-cell biocatalysts, due to their challenging expression and purification, the recent discovery of soluble LAOs with high expression yields and broad substrate scope has repositioned LAOs as attractive alternatives for the selective oxidation step, especially for applications requiring purified enzymes or immobilized biocatalysts. When combining enzymatic oxidations with non-selective chemical reductions by ammonia-borane, complete deracemization of phenylalanine and its analogues can be achieved; however, a large excess (~40 equiv.) of the reducing agent is required (Figure 19, routes C2–C4).¹⁰³ This limitation has propelled the development and use of enzymatic alternatives, integrating the DAADH and/or DAAT-mediated reductive amination within efficient enzymatic cascades for accessing D-phenylalanines (Figure 19, routes A1–A3, B1–B4, and B1–B4' and Sections 5.3, 5.4, and 5.5). Thus, the enzymatic deracemization or stereoinversion cascades start from the racemic or L-phenylalanines and combine L-selective enzymatic oxidation with the D-selective reduction of phenylpyruvate, while the cofactor or cosubstrate regeneration is also ensured using auxiliary enzymes. In an alternative chemo-enzymatic approach, the highly accessible cinnamic acids are hydroaminated by PALs of decreased L-selectivity, resulting in mixtures of D,L-phenylalanines, which by deracemization through the L-selective LAAD-deamination coupled with

chemical, non-selective reduction, provided an *in situ* dynamic kinetic resolution-type process that yielded D-phenylalanines (Figure 19, routes C1–C4 and Section 5.6).

5.1. L-Amino Acid Deaminases (LAADs) in the Deracemization/Stereoinversion of Phenylalanines. L-Amino acid deaminases (LAADs), classified under L-amino acid oxidases (LAOs, EC 1.4.3.2), catalyze the stereospecific oxidative deamination of natural L-amino acids to generate the corresponding α -keto acids and ammonia. The electrons from the FADH₂ cofactor, reduced during the reaction, are transferred to a cytochrome protein within a membrane-associated process. Notably, due to their membrane-bound nature, the purification of LAADs is challenging, with the issues related to their expression, structural characterization, and biotechnological applications being well reviewed.¹⁰⁴ Accordingly, herein we highlight the latest advances in their expression and provide details of their activity toward phenylalanines, as well as related protein engineering efforts.

LAADs have been found exclusively in *Proteus* bacterial species, which express two different types of LAADs, sharing a sequence identity of ~57%. Type I LAADs preferentially oxidize aromatic amino acids, including L-Phe, while type II LAADs primarily deaminate basic L-amino acids, such as L-Arg and L-His.^{104,105} To date, four recombinant LAADs have been expressed and characterized, the type I LAADs from *P. mirabilis* and *P. myxofaciens* (*Pmir*LAAD and *Pma*LAAD, respectively) and the type II LAADs from *P. mirabilis* and *P. vulgaris* (*PmI*LAAD and *Pv*LAAD, respectively).^{103,105–111} The type I *Pmir*LAAD, uniformly abbreviated in this study, in other works has been abbreviated as *Pmi*LAAD¹⁰⁶ or *Pm*LAAD.¹¹²

The *Pmir*LAAD, when expressed with the maltose-binding protein (MBP) fusion tag in *E. coli*, provided a soluble protein fraction. However, the cell lysate showed higher specific activity toward L-Phe (0.17 U/mg) than the purified MBP-*Pmir*LAAD (0.025 U/mg), or the cell lysate of the non-tagged

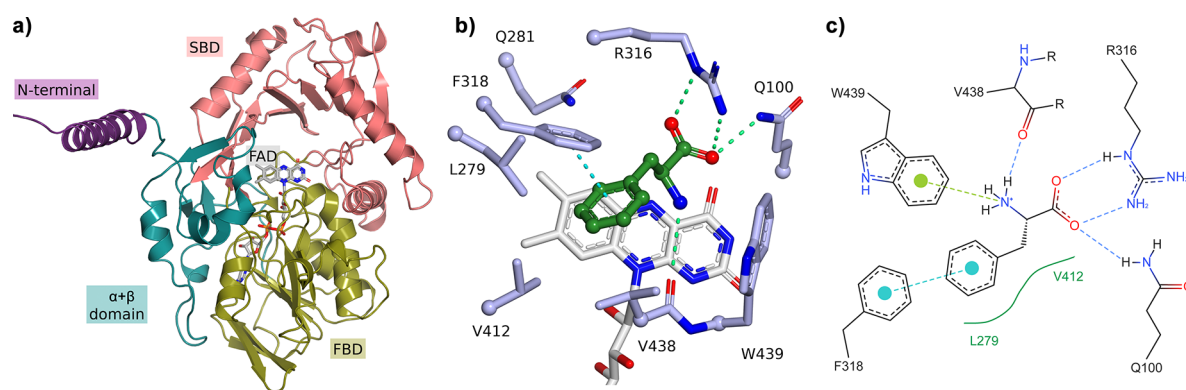


Figure 20. (a) Structural features of LAADs highlighting the N-terminal transmembrane α -helix and the α , β -insertion module, contributing to the active site entrance near the substrate binding domain (SBD) (PDB: 5FJM); (b) The binding model of L-phenylalanine in the catalytic site of *PmaLAAD* (PDB: 5FJN) obtained by docking with Autodock Vina following the reported data;¹¹⁰ (c) 2D diagram of the molecular interaction between catalytic residues of *PmaLAAD* and L-Phe.

PmirLAAD (0.076 U/mg), while the purified *PmirLAAD*, after removing the fusion tag, showed no activity.¹⁰⁹ Using MBP-*PmirLAAD* cell lysate at a concentration of 50 mg/mL, full conversion of 100 mM L-Phe was enabled in a 6 h reaction time.¹¹¹

In terms of productivity, the purified form of type I *PmirLAAD* achieved the maximum productivity value of 1.04 g·L⁻¹·h⁻¹ for phenylpyruvic acid, with a specific activity of 1.02 U/mg and 86.7% mass conversion rate. When using its more accessible, whole-cell biocatalyst form, the production of PPA remained high, with 0.55 g·L⁻¹·h⁻¹ productivity, specific activity of 0.013 U/mg, and an 82.5% mass conversion rate.¹⁰⁹ However, substrate inhibition limited the optimal concentration of the L-Phe substrate to 3–4 g/L.¹⁰⁹ To further optimize the deamination of phenylalanine, *PmirLAAD* was expressed in engineered *E. coli*, in which the *tyrB*, *aspC*, and *ilvE* genes of the aminotransferases that participate in the PPA degradation have been deleted. Thus, the cellular degradation of L-Phe was reduced from the initial 110 mg·L⁻¹·g⁻¹ dry cells to 10 mg·L⁻¹·g⁻¹, improving the PPA titer yield from 3.3 to 3.9 g/L.¹¹³ The error-prone PCR of *PmirLAAD* revealed mutations of residues D165, S179, F236, and L336, improving the catalytic efficiency. Saturation mutagenesis at these positions resulted in the most effective D165K/F263M/L336M variant, which when used in the engineered *E. coli*, offered a PPA-titer of 10 g/L, a near complete conversion of L-Phe. In a fed-batch variant of the procedure, with L-Phe fed in every hour, the substrate inhibition was also alleviated, affording PPA production of 21 ± 1.8 g/L.¹¹³ Furthermore, the supply of FAD was identified as a limiting step in *PmirLAAD*-driven catalysis within the engineered *E. coli*. By the fine-control of the expression level of *ribH*, *ribC*, and *ribF* genes involved in FAD biosynthesis and by the overexpression of formate dehydrogenase (FDH) and NADH oxidase (NOX) for improved FAD/FADH₂ regeneration, the PPA production could be further increased to 31.4 g/L.¹¹⁴

The rational engineering of *PmirLAAD* for enhanced deamination of L-Phe used the homology model of the thermostable, epPCR-derived F93S variant that was built using as template the crystal structure of type-II *PvLAAD* (PDB:5HXW¹⁰⁸).¹⁰⁶ First, by an Ala-scan of eight residues with an occurrence frequency below 60%, the activity-modulator ones were revealed, followed by their NNK-randomization.¹⁰⁶ The best performing F93S/P186A/

M394V/F184S variant showed a 6.6-fold increased specific activity toward L-Phe (Table 3) and provided an effective kinetic resolution of D,L-Phe.¹⁰⁶ Molecular docking indicated a negative correlation between the enzyme activity and the distance between the hydrogen from the C α of the substrate and the cofactor's N5-nitrogen.¹¹⁵ In the case of L-Phe, hydrophobic interactions and van der Waals forces between the substrate channel and the side chain of L-Phe were predicted to affect this distance. The Ala-scan of ten substrate-channel related residues led to the identification of the sextuple variant T105A/D144A/E145A/E340A/S412A/E417A, with 155–165% relative activities for the bulkier substrates, such as L-Phe, when compared to the *wild-type* *PmirLAAD* (Table 3). The orientation of the docked L-Phe within the variant significantly differed from that within the *wild-type*, with the corresponding distance shortened by 0.4 Å and L-Phe favorably interacting with K146, A340, and F317. Using *E. coli* cells harboring plasmids with three copies of the sextuple variant resulted in a 36% and 21% increase of conversion values for L-Phe and L-Tyr, respectively.¹¹⁵ The scale-up to a 5 L reactor resulted in a space-time yield of 8.59 g L⁻¹·h⁻¹ for L-Phe deamination, achieving a high 94.6% conversion in a 12 h reaction time.¹¹⁵

Another study, focusing on expanding the substrate tolerance of type I *PmirLAAD*, docked seven L-amino acids into the homology model of *PmirLAAD* and selected 17 sites, involved in substrate binding, for the Ala-scan.¹¹⁶ The Ala-variants of residues F96, Q278, and E417 showed an activity enhancement toward several L-amino acids, leading to the SM-randomization at these sequence positions. The most active variants, E417A and E417R, showed a 5.6- and 3.9-fold activity increase toward L-Phe compared to the *wt-PmirLAAD*.¹¹⁶ Supposedly, the mutations expanded the substrate channel and removed the electrostatic barriers provided by residue E417.

The product inhibition of the *PmirLAAD*-catalyzed deamination of L-Phe was also alleviated by protein engineering. An Ala-scan of 17 residues from eight loops of the product (PPA) binding site revealed variant E145A/L341A with a 3.8-fold reduction in product inhibition and a 1.3-fold increase of catalytic efficiency in comparison to the *wild-type*. The engineered variant enabled an 81.2 g/L PPA production within a 16 h reaction time.¹¹²

In the case of type I *PmaLAAD*, the highest deamination activities for L-Phe of 14.7 and 15.9 U/mg were obtained upon

Table 4. Specific Activity and Kinetic Parameters (K_M , k_{cat} , k_{cat}/K_M) for the Recombinant LAAO Variants of Different Origins, Purified/Treated with Different Procedures Employing or Not Employing Affinity Tags (for Substrate Numbering, see Figure 19)^a

enzyme/variant/affinity tag		substrate	S.A. ^b (U/mg)	K_M (mM)	k_{cat} (s ⁻¹)	k_{cat}/K_M (s ⁻¹ /mM)
RsLAAO	<i>wild-type</i> MBP/His ₉	L-1a (L-Phe) ¹²⁷	0.13	6.80	0.16	0.02
		L-1a (L-Phe) ¹²⁸	0.02	—	—	—
		L-1an ¹²⁷	0.13	11.70	0.16	0.01
	S2A/T56A/A58S/T204A/K322A/M576S MBP truncated ¹²⁸	L-1a (L-Phe)	0.02	—	—	—
	<i>wild-type</i> SDS-treated MBP/His ₉ ¹²⁷	L-1a (L-Phe)	9.70	2.30	12.20	5.30
HcLAAO	<i>wild-type</i> untreated/His ₆ ¹²⁹	L-1an	8.10	13.90	10.20	0.70
		L-1a (L-Phe)	0.72	0.26	0.83	3.14
		L-1a (L-Phe)	18.90	0.48	21.90	45.20
	<i>wild-type</i> activated at pH = 3/His ₆ ¹²⁹	L-1a (L-Phe)	3.25	0.07	—	—
	<i>wild-type</i> untreated/His ₉ ¹³⁰	L-1o	2.86	1.85	—	—
		L-1a (L-Phe)	12.11	0.07	—	—
		L-1ao	9.21	1.12	—	—
	<i>wild-type</i> activated at pH = 3/His ₉ ¹³⁰	L-1a (L-Phe)	19.00	n.d.	n.d.	n.d.
	<i>wild-type</i> His ₆ truncated ¹³¹	L-1al	2.10	n.d.	n.d.	n.d.
	E288H His ₆ truncated ¹³¹	L-1a (L-Phe)	20.00	n.d.	n.d.	n.d.
AncLAAO	N1/His ₆ ¹³³	L-1al	3.90	n.d.	n.d.	n.d.
		L-1a (L-Phe)	7.70	3.47	25.54	7.36
		(±)-1c	n.d.	3.54	25.90	7.11
		(±)-1d	11.40	2.22	29.67	13.33
		(±)-1e	14.50	0.90	30.68	34.13
		(±)-1f	5.20	4.10	25.11	6.13
		(±)-1h	11.30	n.d.	n.d.	19.37
		(±)-1i	8.00	n.d.	n.d.	n.d.
		(±)-1j	0.33	n.d.	n.d.	n.d.
		(±)-1n	n.d.	2.55	25.48	9.96
		(±)-1o	n.d.	2.86	33.20	11.61
		(±)-1p	n.d.	0.69	20.39	29.55
		(±)-1q	6.70	1.70	20.44	11.96
		(±)-1s	n.d.	0.59	25.47	42.60
		(±)-1v	n.d.	n.d.	n.d.	23.31
		(±)-1u	n.d.	1.05	26.32	25.91
	N4/His ₆ ¹³⁴	(±)-1x	n.d.	5.30	6.14	1.15
		(±)-1y	n.d.	4.14	0.98	0.24
		(±)-1z	3.3	n.d.	n.d.	n.d.
		(±)-1ac	n.d.	n.a	n.a	n.a
		(±)-1ad	n.d.	n.d.	n.d.	0.78
		(±)-1af	n.d.	1.25	32.00	25.66
		(±)-1ag	n.d.	1.21	26.55	21.91
		(±)-1ai	n.d.	8.20	12.12	1.48
		(±)-1aj	10.30	n.d.	n.d.	n.d.
		(±)-1al	0.21	n.d.	n.d.	n.d.
	N4-Y567F/His ₆ ¹³⁴	(±)-1a ((±)-Phe)	7.60	n.d.	n.d.	n.d.
		(±)-1d	10.20	n.d.	n.d.	n.d.
		(±)-1i	12.80	n.d.	n.d.	n.d.
		(±)-1j	0.38	n.d.	n.d.	n.d.
		(±)-1q	9.70	n.d.	n.d.	n.d.
		L-1a (L-Phe)	n.d.	3.20	16.70	5.20
		N4-D249F/Q536 V/Y567F/His ₆ ¹³⁴	n.d.	23.9	4.6	0.19
		N4-D249A/Q536G/Y567F/His ₆ ¹³⁴	n.d.	1.30	16.70	12.80
HTAncLAAO ¹³⁵	His ₆	L-1a (L-Phe)	n.d.	3.60	28.50	7.9
		L-1a (L-Phe)	n.d.	0.30	8.70	29.00
HTAncLAAO2 ¹³⁶	His ₆	L-1a (L-Phe)	n.d.	0.07	14.5	204
RoLAAO ¹³⁷	His ₆	L-1a (L-Phe)	n.d.	0.02	20.9	814
		Y226H/D227H/Y371L/A466C/W467A/His ₆	n.d.	0.01	240.2	22785

^aKinetic parameters and specific activities were determined under the reported assay conditions (see references in the table). ^bS.A.: specific activity; one unit (U) was defined as the amount of enzyme consuming 1 μ mol of substrate per minute. His_{6/9}: His-tag containing either 6 or 9 histidine residues.

Table 5. Purification Yields of Ancestral LAAOs and Their Use in Preparative Scale Deracemizations of Racemic Phenylalanines and Phenylglycine^a

enzyme		bacterial host	enzyme purification yield (mg/L ferment)	substrate	enzyme amount (mg)	scale (mg)	yield (%)	ee (%)	
AncLAAO ¹³²	N1	<i>E. coli</i> BL21 (DE3)	50.7	(±)-1z	7	183	—	>99	
				(±)-1i		210	—	>99	
				(±)-1aj		219	—	>99	
				(±)-1am		151	—	>99	
	N4	<i>E. coli</i> BL21 (DE3)	55.1	(±)-1a ((±)-Phe)	3	166	—	94	
				(±)-1i		210	92	>99	
				(±)-1d		2	195	—	>99
				(±)-1j			180	—	97
				(±)-1q			183	86	>99
HTAncLAAO ¹³⁵	<i>E. coli</i> BL21 (DE3)	53.9	(±)-1a ((±)-Phe)	0.4	165	—	>99		
			(±)-1i		183	96	>99		
			(±)-1q		210	87	>99		

^aThe reactions were performed under the reported conditions (see references within the table).

preincubation with detergents, such as SDS or *N*-laurylsarcosine, and in the presence of the electron transfer reactant phenazine methosulfate (PMS).¹¹⁷ The recombinantly expressed, purified *Pma*LAAD, activated by the addition of exogenous membranes, showed a higher specific activity of 0.51 U/mg toward L-Phe under optimized conditions, which is still lower than the evolved D165K/F263M/L336M *Pmir*-LAAD.¹¹⁸ The *Pma*LAAD exhibited broad substrate tolerance, with high activity toward several aromatic substrates, including L-4-nitrophenylalanine, 3-pyridyl-alanine, L-DOPA, homophenylalanine, and L-1-naphthylalanine. In the case of L-4-nitrophenylalanine, the enzyme displayed an ~4-fold higher specificity constant ($k_{\text{cat}}/K_{\text{M}}$) compared to L-Phe (Table 3).¹¹⁸ To test *Pma*LAAD on a preparative scale, 130 mg of L-4-nitrophenylalanine was fully converted to the D-enantiomer ($ee > 99\%$), using 7.5 U enzyme and 62.5 mM *tert*-butylamine borane complex.¹¹⁸

While the challenging structural characterization of LAADs hindered their rational engineering, type I *Pma*LAAD, lacking the putative *N*-terminal transmembrane helix (residues 8–27) required for membrane association, was successfully crystallized (PDB: 5FJM and 5FJN).¹¹⁰ Its spectral properties and monomeric fold resembled those of the full-length enzyme, but it was not activated by the presence of *E. coli* membranes or cells, likely due to the poor electron transfer caused by its membrane-association inability.¹¹⁰ The overall fold of the truncated *Pma*LAAD resembled those of amino acid oxidases (AAOs),¹¹⁰ including a FAD-binding domain (FBD) and a substrate binding domain (SBD). Notably, specific for LAADs, the presence of the putative *N*-terminal transmembrane α -helix, ensuring its membrane association, and the presence of an additional α/β -insertion module, closely positioned to the transmembrane helix and interconnected with the SBD, formed a significant portion of the active site entrance (Figure 20a). Using the anthranilate, a substrate analogue-bound structure of *Pma*LAAD (PDB: 5FJN), the molecular interactions with phenylalanine (Figure 20b,c) and bulkier substrates, such as L-DOPA or L-1-naphthylalanine (L-1Nal), were predicted.^{104,110} The binding model of L-Phe suggests residues L279, R316, F318, V412, and W439 interact with the substrate side chain (Figure 20b) and influence substrate specificity. After multiple rounds of saturation mutagenesis at the above selected positions, the best performing variant

F318A/V421A/V438P, with an ~7-fold increase in catalytic efficiency for L-1Nal, also contained an unpredicted mutation at position 438, likely introduced by PCR-amplification errors.¹¹⁹ In the case of the improved variant, the ratio between the specificity constant for L-1Nal and L-Phe was ~110-fold higher compared to the wild-type enzyme, highlighting a significant increase in activity toward naphthyl-substituted alanines (Table 3). Additionally, variant F318V/V412L was also identified from the created libraries, presenting an ~1.6-fold increase in activity toward L-Phe.¹¹⁹

Regardless of the deamination activity of type-II LAADs toward phenylalanines, type II *Pml*LAAD shows lower reaction velocities (v_{max} of 0.73 μmol phenylpyruvic acid $\text{min}^{-1}\text{mg}^{-1}$) and substrate affinity (K_{M} of 31.5 mM)^{105,107} than type I *Pma*LAAD (v_{max} of 1.64 μmol PPA $\text{min}^{-1}\text{mg}^{-1}$ and K_{M} of 26.2 mM)¹⁰⁹ (Table 3). Notably, no data have been reported on the deamination of phenylalanines by the structurally characterized type II *Pv*LAAD.¹⁰⁸

5.2. L-Amino Acid Oxidase (LAAO)-Mediated Stereoselective Oxidation of Phenylalanines. In the case of L-amino acid oxidases (LAAOs, EC 1.4.3.2), in contrast to LAADs (Section 5.1), during the oxidation of the L-amino acid substrates, the reduced FADH₂ is reoxidized by molecular oxygen while producing hydrogen peroxide. For several decades the biocatalytic applications of LAAOs remained limited due to well-reviewed challenges,^{120,121} including their extremely low recombinant expression levels,^{122,123} narrow substrate tolerance,^{107,124–126} and lack of screening assays required for directed evolution approaches. Recent advances, highlighted in this Review, provided access to LAAOs of broad aromatic substrate scope and high expression levels, opening new perspectives for their synthetic applications.

The LAAO from fungus *Rhizoctonia solani* (RsLAAO) was expressed in *E. coli* with a removable maltose-binding protein (MBP) solubility tag,¹²⁷ followed by activation *via* treatment with 0.025% SDS (Table 4). Despite being isolated in low yield (4.4 mg/L ferment), RsLAAO converted hydrophobic L-amino acids with high relative activity, including L-Phe, as well as its methyl ester (Table 4). To enhance the soluble expression of RsLAAO, 108 out of its 645 residues were selected for mutation, replacing hydrophobic amino acids with serine and hydrophilic ones with alanine.¹²⁸ Logistic regression modeling on the activity values of the 108 single mutants identified 6

effective mutation sites improving LAAO solubility, while extending the mutational analysis to all 645 residues, an additional 52 effective sites were identified. The 6- and 58-point mutant variants of RsLAAO showed a 2.6- and 4.2-fold increase in solubility in comparison to the *wild-type* variant. The sextuple mutant S2A/T56A/A58S/T204A/K322A/M576S RsLAAO retained a specific activity of ~ 0.0243 U/mg, similar to that of the *wild-type*, while the 58-mutation bearing variant was inactive, supposedly due to mutations within the FAD binding domain.¹²⁸

The LAAO from *Hebeloma cylindrosporum* (HcLAAO), expressed in *E. coli*, was activated under acidic pH or freezing conditions¹²⁹ and exhibited a specific activity 2-fold higher for L-Phe than that of SDS-activated RsLAAO, while also transforming the methyl esters of L-amino acids (Table 4). Its expression in *P. pastoris* ensured higher cell densities and 50-fold higher activity, achieving 9200 U/L ferment, while the isolated enzyme retained a similar activity to the one expressed in *E. coli*.¹³⁰ By rational design, catalytic residue E288, critical for transforming substrates with basic side chains and hindering the transformation of negatively charged substrates, was targeted for replacement. Variant E288H exhibited a 1.85-fold activity increase for L-2-naphthylalanine (~ 3.9 U/mg) compared to the *wild-type* (~ 2.1 U/mg), while its activity for L-Phe remained unchanged (19–20 U/mg).¹³¹

By exploring paralogous genes of the native L-arginine oxidase (AROD) from *Oceanobacter kriegii*, the LAAO from *Pseudomonas piscicida* and six other homologous sequences were identified and selected for ancestral sequence reconstruction (ASR). In a breakthrough, the resulting ancestral LAAO (AncLAAO) could be expressed in *E. coli* with a high production yield of 50 mg (672 U)/L (Table 5).¹³²

The AncLAAO, abbreviated as variant N1, displayed a broad substrate scope, transforming 13 L-amino acids, both hydrophilic and hydrophobic ones, with k_{cat} values ranging from 6.0 to 33.0 s⁻¹, comparable to those of other reported LAAOs (Table 4). Substrate profiling revealed that monosubstituted phenylalanines, with either electron-donor or electron-withdrawing substituents, are all accepted as substrates.¹³³ Notably, *para*- and *meta*-substituted phenylalanines exhibited high turnover numbers, comparable to or even exceeding the deamination rate of L-Phe. In contrast, *ortho*-substituted analogues showed lower turnover numbers, with the activity decreasing as the size of the substituent increased, suggesting steric hindrance within the catalytic site. Among phenylalanines with multiple ring substituents, AncLAAO-N1 was inactive toward 2,4-dimethoxy-Phe, but was able to transform *meta*- and *para*-disubstituted derivatives, as well as 3,4,5-trimethoxy-Phe.¹³³

AncLAAO-N1, combined with the chemical reductant NH₃·BH₃, enabled the deracemization of 18 phenylalanines, achieving complete conversion to D-enantiomers within 24 h, except for the non-transformed *p*-NH₂-phenylalanine (Table 4).¹³² When performed at ~ 200 mg-scale, the deracemization of 2-F-Phe, 3-F-Phe, 4-NO₂-Phe, and 3,4,5-trifluoro-Phe using 7 mg of AncLAAO-N1 and 150 mM NH₃·BH₃, quantitatively yielded the corresponding D-phenylalanines. Since the enzyme activity significantly decreased to <15% of the original value after 60 min of incubation at 30 °C, another ancestral variant, AncLAAO-N4, with an optimal temperature of 50 °C and >55% relative activity retained at 65 °C, was also employed within the preparative-scale deracemizations, reducing the required biocatalyst amount to 2–3 mg/reaction (Table 5).¹³⁴

The hyper-thermostable AncLAAO (HTAncLAAO), obtained by combining the ASR approach with sequence data mining, showed a narrower substrate scope, transforming only seven amino acid substrates, with the highest relative activity observed for L-Phe (Table 4).¹³⁵ However, its high thermal and operational stability, with a T_{50}^{10} value of 95 °C, assessed within the oxidation of L-Met, and the >95%, 60%, 30%, and 10% activity retained after a 1 week incubation at 30, 40, 50, and 60 °C, respectively, allowed the use of only 0.4 mg (2 U) of purified enzyme for the ~ 200 mg-scale deracemization of D,L-Phe, 3-F-D,L-Phe, and 4-NO₂-D,L-Phe. As is typical for the oxidations with LAAOs, the additional use of catalase (~ 20 kU) to decompose the generated peroxide was also necessary to obtain in high 87–96% yields the D-phenylalanines (Table 5). A distinct hyperthermostable AncLAAO (HTAncLAAO2), when compared to HTAncLAAO, showed ~ 1.7 - and 7-fold enhancement of the turnover number and specificity constant, respectively, for L-phenylalanine (Table 4).¹³⁶ The crystal structure of the ligand-free and L-Gln, L-Phe, and L-Trp complexed forms of AncLAAO-N5 (PDB: 7C4K, 7C4L, 7C4N, and 7C4M, respectively), revealed the substrate recognition and reaction mechanism of AncLAAOs.¹³⁴ Residues R89, Y447, G570, and W571 ensure the fixation of the –COOH and –NH₂ groups of the L-amino acid, while the aromatic side chain of L-Phe forms hydrophobic interactions with L247, V535, and F231 (Figure 21a). Within the reaction mechanism, the oxidation at the α -carbon of L-Phe is proposed to occur *via* deprotonation of the protonated –NH₂ group by a water molecule, with a simultaneous transfer of the hydride anion from the C α of L-Phe to the N5 of the FAD cofactor.

Rational design of *Rhodococcus opacus* LAAO (RoLAAO), one of the first explored LAAOs of broad substrate

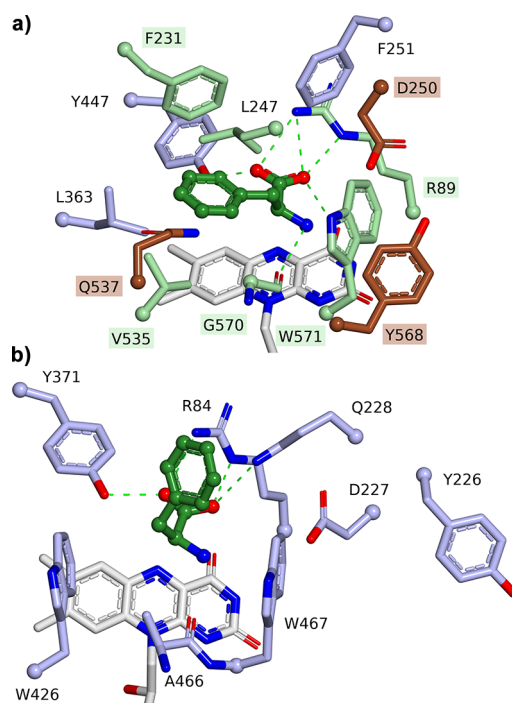


Figure 21. Active site orientation of the L-Phe (a) in AncLAAO-N5 (PDB: 7C4N) and the residues subjected to site-specific (green) and/or saturation (brown) mutagenesis, leading to variants of enhanced activity toward L-Phe and (b) in RoLAAO (PDB: 2JB2), highlighting the residues selected for mutagenesis.¹³⁷

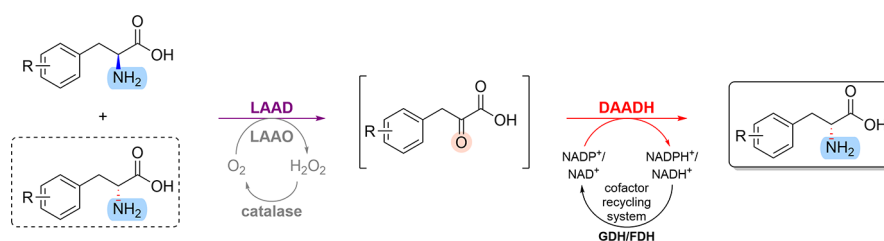


Figure 22. LAAD (LAAO)/DAADH deracemization cascade consisting of the deamination step mediated by LAAD (or LAAO coupled with catalase) and stereoselective reductive amination catalyzed by DAADH, along with the corresponding cofactor regeneration system (GDH/FDH).

Table 6. Stereoinversion Cascades Producing D-Phenylalanines, with Conversion (conv), Enantiomeric Excess (ee), Yield, and Productivity Values

product	cascade	conv (%)	ee (%)	yield/productivity
D-Phe	<i>PmirLAAD</i> ^a / <i>CgDAADH</i> ^{a,39}	—	98	76% ^f
	<i>PmirLAAD</i> ^{a,e} / <i>W121A/R181S/H227I PvDAPDH</i> ^a / <i>BmGDH</i> ^{a,53}	96.3	>99	1.92 g/L/h
	<i>PmirLAAD</i> ^a / <i>H227 V StDAPDH</i> ^b / <i>BsFDH</i> ^{b,140}	>99	99	2.20 g/L/h
	<i>PmirLAAD</i> ^c / <i>StDAPDH</i> / <i>BsFDH</i> ¹⁴¹	>99	99	1.03 g/L/h
	<i>PmaLAAD</i> ^a / <i>BsDAAT</i> ^{a,110}	—	>99	4.15 g/L ^g
	<i>EcGluRA</i> ^d / <i>BsDAAT</i> / <i>CbGDH</i> / <i>CbFDH</i> ¹⁴⁶	>99	>99	1.37 g/L/h
	<i>BtSK-1 GluRA</i> ^d / <i>BsDAAT</i> / <i>CbGDH</i> / <i>CbFDH</i> ⁶⁴	>99	>99	1.66 g/L/h
	<i>AncLAAO-N4</i> ^d / <i>catalase</i> / <i>CgDAADH</i> / <i>BmGDH</i> ¹⁴²	—	>99	54.7% ^f
	<i>PmirLAAD</i> ^a / <i>W121I/R181S/H227I PvDAPDH</i> ^a / <i>BmGDH</i> ^{a,54}	70.7	99	1.18 g/L/h
D-o-Me-Phe	<i>PmirLAAD</i> ^a / <i>CgDAADH</i> ^a / <i>BmGDH</i> ^{a,39}	—	95	83% ^f
	<i>T242G BsDAAT</i> ^a / <i>PmirLAAD</i> ^{a,65}	>99	90	—
D-m-Me-Phe	<i>T242G BsDAAT</i> ^a / <i>PmirLAAD</i> ^{a,65}	>99	96	—
D-p-Me-Phe	<i>PmirLAAD</i> ^a / <i>CgDAADH</i> ^a / <i>BmGDH</i> ^{a,39}	—	>99	79% ^f
	<i>PmirLAAD</i> ^c / <i>StDAPDH</i> / <i>BsFDH</i> ¹⁴¹	67.4	—	—
	<i>T242G BsDAAT</i> ^a / <i>PmirLAAD</i> ^{a,65}	>99	93	—
D-o-Cl-Phe	<i>PmirLAAD</i> ^c / <i>StDAPDH</i> / <i>BsFDH</i> ¹⁴¹	>99	>99	—
	<i>T242G BsDAAT</i> ^a / <i>PmirLAAD</i> ^{a,65}	>99	98	—
D-m-Cl-Phe	<i>PmirLAAD</i> ^c / <i>StDAPDH</i> / <i>BsFDH</i> ¹⁴¹	>99	>99	—
	<i>T242G BsDAAT</i> ^a / <i>PmirLAAD</i> ^{a,65}	>99	99	—
D-p-Cl-Phe	<i>PmirLAAD</i> ^c / <i>StDAPDH</i> / <i>BsFDH</i> ¹⁴¹	>99	>99	—
(D-p-OH-Phe) D-Tyr	<i>PmirLAAD</i> ^c / <i>StDAPDH</i> / <i>BsFDH</i> ¹⁴¹	45.3	>99	—
	<i>EcGluRA</i> ^d / <i>BsDAAT</i> / <i>CbGDH</i> / <i>CbFDH</i> ¹⁴⁶	>99	>99	1.71 g/L/h
	<i>PmirLAAD</i> ^a / <i>W121I/R181S/H227I PvDAPDH</i> ^a / <i>BmGDH</i> ^{a,54}	83.9	99	1.43 g/L/h
D-m-MeO-Phe	<i>T242G BsDAAT</i> ^a / <i>PmirLAAD</i> ^{a,65}	>99	98	—
D-p-MeO-Phe	<i>PmirLAAD</i> ^a / <i>CgDAADH</i> ^a / <i>BmGDH</i> ^{a,39}	—	>99	76% ^f

^aApplied as whole-cell biocatalysts. ^bApplied as a purified enzyme. ^cOne-cell assembly. ^dCell-free multienzyme system. ^eWith two copies of *PmirLAAD*. ^fIsolation yield of 100 mg-scale experiment. ^gProductivity in g/L (reaction times not provided within reported data).

specificity,¹³⁸ with an available crystal structure with L-Phe (PDB: 2JB2) (Figure 21b),¹³⁹ led to the development of variants transforming L-Phe to phenylpyruvic acid with a conversion $\geq 95\%$ and a yield of $\sim 95 \text{ g} \cdot \text{L}^{-1}$ when operating as a whole-cell biocatalyst in a 5 L reactor over a 12–24 h reaction time.¹³⁷ To reduce the energy barrier of the transition states, mutations Y226H, D227H, and Q228H were proposed to enhance the proton abstraction ability from the substrate's $-\text{NH}_2$ group within the first step of the reaction mechanism. To reduce the energy barrier in the subsequent step, the replacement of large-volume residues from the substrate-binding pocket was targeted, thus releasing the steric hindrance of the substrate's orientation and decreasing the distance from the C α of the substrate to the N5 of FAD, thereby facilitating the hydride transfer.

From docking of transition states and MD simulations, residues R84, Y371, W426, and W467 were selected as sites for saturation mutagenesis (Figure 21b). Finally, combining the mutations of the most improved variants, provided Y226H/D227H/Y371L/A466C/W467A *RoLAAO* that, compared to

the wild-type enzyme, showed a 2.4-fold reduced K_M value, an 11.5-fold increased k_{cat} value, and a 28.2-fold increased specificity constant (k_{cat}/K_M) within the oxidative deamination of L-Phe (Table 4).¹³⁷ In comparison to the high protein isolation yields of *AncLAAOs*, the expression issues still persisted for *RoLAAO*. Its purified form was obtained by the expression in *E. coli* with the removable MBP fusion tag, which was required for protein solubility.¹³⁷

5.3. Enzyme Cascades Involving DAADH-Mediated Reductive Amination. As engineered DAADHs emerged as alternatives for the reductive amination of aromatic keto acids, the enzymatic whole-cells cascade consisting of *PmirLAAD*, *CgDAADH*, and the cofactor-recycling glucose dehydrogenase (GDH) (Figure 22) was tested for the deracemization or stereoinversion of various racemic or L-arylalanines, producing D-phenylalanines with high enantiomeric excess values and yields (Table 6).³⁹

The cascade of engineered W121A/R181S/H227I *PvDAPDH*, *PmirLAAD*, and GDH from *Bacillus megaterium* (*BmGDH*) provided the one-pot, quantitative stereoinversion

of L-Phe into D-Phe (>96% conversion, $ee > 99\%$). At 3 L-scale using *E. coli* cells harboring two copies of the *PmirLAAD* encoding gene and one copy of the gene of the *PvDAADH* variant and of *BmGDH* resulted in a 57.8 g/L titer-yield for D-Phe after a 30 h reaction time.⁵³ The cascade performed with a similar variant, W121I/R181S/H227I of *PvDAPDH*, provided enantiopure forms of D-Phe, D-Tyr, D-phenylglycine, and D-homophenylalanine, among other D-AAAs; however, lower titer yields of 28.3, 33.6, 14.8, and 29.4 g/L, respectively, were registered after a 24 h reaction time.⁵⁴ Lower titer yields of 13.2 g/L D-Phe were also registered for the cascade that combined purified forms of H227V *StDAPDH* and formate dehydrogenase from *Bacillus simplex* (*BsFDH*) with the *PmirLAAD* whole-cell biocatalyst.¹⁴⁰ However, when using wild-type *StDAPDH*, *BsFDH*, and *PmirLAAD* as a one-cell assembly, a higher titer yield of 24.7 g/L D-Phe was obtained after 24 h. The later cascade was also explored for the stereoinversion of various L-amino acids, including *o*-, *m*-, and *p*-chloro-substituted phenylalanines, into D-phenylalanines, achieving complete conversions.¹⁴¹ In cases of L-Tyr and L-4-methyl-Phe, moderate conversions of 45.3% and 67.4%, respectively, were registered (Table 6). In a four-enzyme cascade, alongside *CgDAADH/BmGDH*, the use of *AnCLAAD-N4* as an alternative to LAAD was tested, with the additional use of catalase for removing the produced H_2O_2 .¹⁴² In the optimal setup, using cell-free extract biocatalysts and 10 mM solutions of L-amino acids, the enantiopure D-Phe and D-Trp were produced in 48 h; however, at the preparative-scale, the stereoinversion of L-Phe and deracemization of D,L-4-Br-Phe and D,L-3-F-Phe provided isolation yields of only 54.7%, 6.9%, and 1.3%, respectively.¹⁴²

5.4. Enzyme Cascades Involving DAAT-Mediated Reductive Amination. The whole-cell cascade developed by Monsanto Co. coupled the *PmaLAAD*-catalyzed deamination of racemic amino acids with the *BsDAAT*-mediated reductive amination, while ensuring the regeneration of the D-amino donor by an amino acid racemase (AAR), most frequently alanine, glutamate, or aspartate racemase.⁷⁰ When using D-aspartate as the amino donor, the succinate byproduct of the reductive amination spontaneously decarboxylates to pyruvate, shifting the equilibrium toward D-Phe production (Figure 23).¹⁸ The process has been applied industrially for the production of several D-amino acids, including D-Phe and D-Tyr.¹⁴³

Employing the cascade in modified *E. coli* cells, with phenylpyruvate provided by an external feed or via the LAAD-deamination of the intracellularly produced L-Phe, and with the

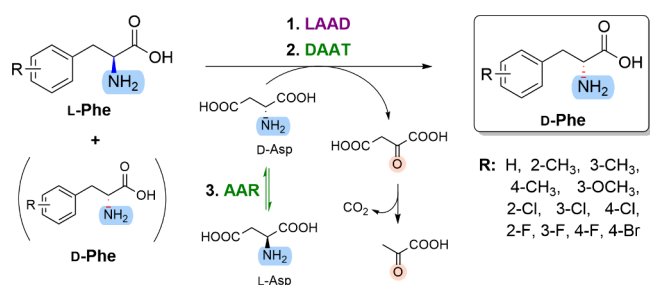


Figure 23. LAAD/DAAT/AAR deracemization cascade involving the LAAD-catalyzed deamination, the DAAT-mediated reductive amination, and the aspartate racemase catalyzed generation of the D-amino donor.

amino donor D-Ala ensured by the alanine racemase (AlaR) from L-Ala, the YM-1 *BsDAAT* was able to produce the desired D-Phe with a 4.15 g/L titer yield (Figure 24).^{144,145} Under the fermentative conditions, the pyruvate byproduct was catabolized, shifting the equilibrium toward 100% completion.

A similar cascade in the form of a cell-free multienzymatic system composed of glutamate racemase (GluRA), *BsDAAT*, glutamate dehydrogenase (GluDH), and FDH required only small initial amounts of L-Glu and NAD^+ for complete conversions of phenylpyruvates, producing D-Phe in 48 g/L and D-Tyr in 60 g/L titer yields.¹⁴⁶ By using a thermostable GluRA from *Bacillus thermophilus* SK-1, the productivity of D-Phe was increased to 58 g/L.⁶⁴

In stereoinversion/deracemization cascades the engineered T242G DAAT (see Section 5), used as a whole-cell biocatalyst, in combination with *PmirLAAD*, yielded various D-phenylalanines (Tables 6 and 7).⁶⁵ Its synthetic utility was showcased by the preparative deracemization, yielding D-4-fluorophenylalanine. The optimized procedure used an excess of D-aspartate, which after the reaction was removed by D-aspartate oxidase, affording D-4-fluorophenylalanine in 84% isolation yield.⁶⁵ The disadvantage of requiring stoichiometric amounts of the amino donor can be overcome by its *in situ* regeneration through racemases, as demonstrated by the Monsanto process,⁷⁰ and/or by replacing *PmirLAAD* with *PmaLAAD*, which is unable to deaminate L-glutamate or L-aspartate.¹¹⁰ The LAAD/DAAT cascade, when combined with tryptophan synthase (TrpS), served for the synthesis of D-tryptophans, using indoles and serine as the starting materials. The engineered V33G/T242G *BsDAAT* with a 35-fold increased k_{cat}/K_M toward D-Trp derivatives was coupled with TrpS from *Salmonella enterica* and *PmaLAAD* (Figure 25).¹⁴⁷

Notably, the substrate specificity of TrpS was recently unlocked by directed evolution, providing tyrosine synthetase activity,¹⁴⁸ with the perspective for extending this cascade toward D-phenylalanine synthesis.

5.5. Enzyme Cascades Involving Both DAAT- and DAADH-Mediated Reductive Amination. The one-pot DAAT/DAADH cascade, coupled with alcohol dehydrogenase (ADH) for cofactor regeneration, aimed to exploit the advantages of diversity and broad substrate scope of transaminases while overcoming the limitation of their reversible reaction by using DAADHs, which irreversibly catalyze the reductive amination but show a narrower substrate specificity. In this approach, *BsDAAT* ensured the amino transfer from D-Ala to pyruvate, resulting in the desired D-amino acid, while *StDAPDH* recycled the amino donor from the DAAT-produced pyruvate byproduct, also shifting the equilibrium of the transamination step (Figure 26).¹⁴⁹ The ADH from *Thermoanaerobacter brockii* (*TbADH*) ensured the $NAD(P)H$ -recycling using 2-propanol as a cheap cosubstrate (Figure 26).¹⁴⁹

Using purified enzymes as biocatalysts and catalytic amounts of amino donor, along with inexpensive ammonia for its regeneration, D-Phe and D-Tyr were successfully obtained with conversion values >99% (Table 6). The cascade lacking DAAT provided low conversions of <20% for D-Phe and <5% for D-Tyr, supporting the dual role of DAADH in both recycling the amino donor and transforming the substrate into the targeted D-amino acid.

5.6. Enzyme Cascades Involving the PAL-Mediated Hydroamination. By coupling the engineered H359Y *AvPAL*-mediated ammonia addition of electron-deficient

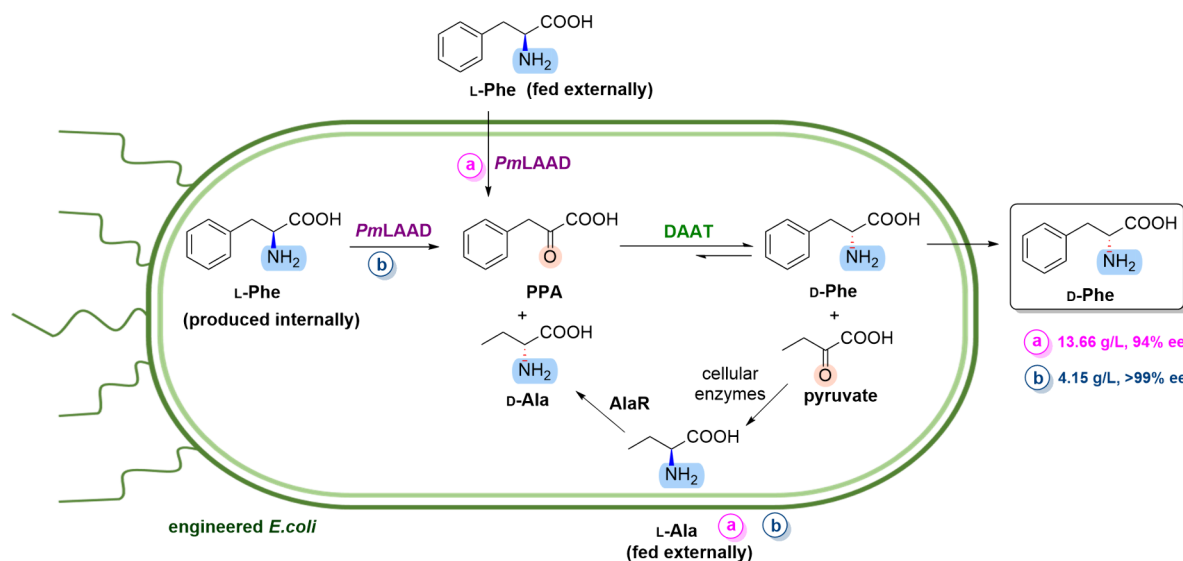


Figure 24. Fermentation-based production of D-phenylalanine using engineered *E. coli* hosting the LAAD/DAAT/AAR cascade, with an external addition (a) of D,L-Ala and L-Phe or (b) of only D,L-Ala.^{144,145} Figure adapted with permission from ref 144. Copyright 1998 Elsevier.

cinnamic acids (see Section 4), with *Pmir*LAAD-deamination and with the subsequent chemical reduction, several D-phenylalanines (Figure 27) were produced with high yields and optical purity (Table 7).⁹⁰

Although the formation of phenylpyruvic acids as side products, through the spontaneous hydrolysis of the imino acid intermediates, slightly reduced the overall yields, the equilibrium of the PAL reaction was pulled by the LAAD-mediated deamination toward the formation of phenylalanines, providing a beneficial effect within the cascade.⁹⁰ Engineered N347A *Av*PAL (see Section 4) was employed in a similar, but sequential, one-pot cascade, also enabling the production of D-phenylalanines with *ee* values of 72–99% (Table 7).⁹¹ As a disadvantage, a large excess of 40 equiv. of ammonia-borane is requested, which was addressed by the fully biocatalytic procedure, where the spontaneous hydrolysis of the imino acid intermediate was coupled with the DAAT-catalyzed transamination.¹⁵⁰ Using whole-cell biocatalysts in a sequential, one-pot process, the preparative synthesis of sitagliptin D-2,4,5-trifluorophenylalanine was performed with 62% yield. The cascade was initiated by the *Av*PAL-mediated hydroamination of a 50 mM 2,4,5-trifluorocinnamic acid solution, followed by a 2-fold dilution of the reaction, while whole-cells of *Pmir*LAAD and engineered T242G YM-1 *Bs*DAAT were added for the complete deracemization in 8 h, with a global reaction time of 20 h. The approach required the additional degradation of the D-Asp amino donor using D-aspartate oxidase from *Bos taurus* (*Bt*DDO).¹⁵⁰ Notably, in both processes, high conversions could be obtained only with substrates bearing electron-withdrawing ring substituents, in which case the production level of D-Phe by PAL-hydroamination became significant. For substrates with electron-donating groups, the L-Phe derivative highly dominates despite the use of variants engineered for increased D-selectivity. Thus, the development of efficient D-selective PALs still remains a challenge.

5.7. Case Study Serving as a Comparison of the Biocatalytic Cascades. The cascades suitable for D-phenylalanine production were tested and compared in terms of productivity and environmental impact, using as case study the synthesis of D-2,3,5-trifluorophenylalanine, precursor for the

antidiabetic sitagliptin (Figure 28).¹⁵⁰ For the reductive amination of the corresponding keto acid two whole-cell cascades were successfully applied: (i) the DAADH/GDH cascade, using the engineered *Cg*DAADH and *Bm*GDH; (ii) the DAAT-based cascade involving T242G *Bs*DAAT and *Bt*DDO. In both cases, complete conversions were achieved in 12 h; however, the *Cg*DAADH/*Bm*GDH cascade enabled the use of higher, 50 mM substrate concentrations and 81% isolation yield, whereas the T242G *Bs*DAAT/*Bt*DDO cascade was limited to 25 mM substrate concentration and 75% yield. With DDO only facilitating product isolation, the DAAT/DDO cascade was accomplished in a two-step telescopic manner, requiring an additional 8 h for the DDO-mediated step. In contrast, the DAADH/GDH cascade could be conducted in a one-pot, one-stage manner using whole cells producing both enzymes. Both systems, when coupled with the *Pmir*LAAD-deamination allowed deracemization of racemic 2,3,5-trifluorophenylalanine, with the *Pmir*LAAD/T242G *Bs*DAAT/*Bt*DDO cascade, affording a product isolation yield of 74% compared to the 79% yield of the *Pmir*LAAD/*Cg*DAADH/*Bm*GDH system.¹⁵⁰

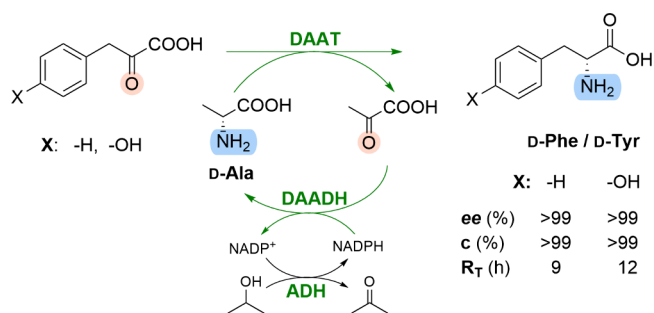
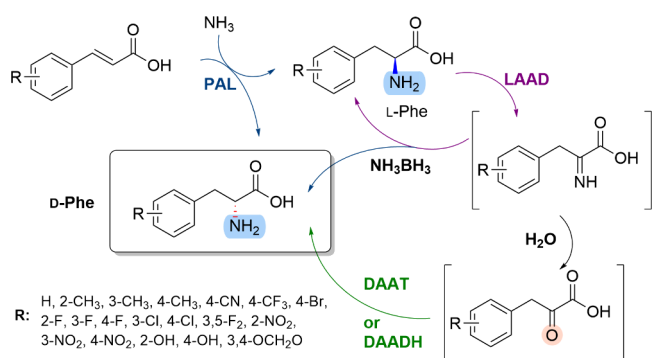
The PAL/LAAD/DAAT/DDO enzymatic cascade (see also Section 5.6) started from the *trans*-2,3,5-trifluorocinnamic acid, which can be accessed by the facile Knoevenagel–Doebner reaction. Using *Av*PAL, *Pmir*LAAD, T242G *Bs*DAAT, and *Bt*DDO, the process, in a 28 h total reaction time, provided the highest overall yield of 62%, calculated from 2,3,5-trifluorobenzaldehyde, including the chemical, Knoevenagel–Doebner reaction step.¹⁵⁰

In all tested procedures the D-2,3,5-trifluorophenylalanine has been obtained with high enantiopurity (*ee* > 99%), although the overall yields varied between 43% and 62% (Table 8 and Figure 28). The environmental footprint of the processes was also estimated based on the calculation of simplified *E*-factors (*sEF*) (Table 8). The LAAD/DAAT-based stereoinversion, despite requiring the lowest number of reaction steps (2 steps), showed the highest value for generated waste and the lowest substrate loading of 25 mM. Its extended LAAD/DAAT/DDO version, which includes five reaction steps, is more attractive for scale-up, allowing high

Table 7. Deracemization Cascades Producing D-Phenylalanines with Conversion (Conv) and Enantiomeric Excess (ee) Values

product	cascade	conv (%)	ee (%)
D-Phe	<i>Pma</i> LAAD ^a / <i>Bs</i> DAAT ^{a,110}	>99 (4.15 ^d)	>99
	T242G <i>Bs</i> DAAT ^a / <i>Pmir</i> LAAD ^{a,65}	>99	>99
	N347A <i>Av</i> PAL ^b / <i>Pmir</i> LAAD ^{b,91}	82	99
	<i>Bs</i> DAAT ^{b,f} / <i>St</i> DAPDH ^b / <i>Tb</i> ADH ^{b,149}	>99	>99
D- <i>o</i> -Me-Phe	N347A <i>Av</i> PAL ^b / <i>Pmir</i> LAAD ^{b,91}	16	89
D- <i>m</i> -Me-Phe	N347A <i>Av</i> PAL ^b / <i>Pmir</i> LAAD ^{b,91}	23	93
D- <i>p</i> -Me-Phe	N347A <i>Av</i> PAL ^b / <i>Pmir</i> LAAD ^{b,91}	12	92
D- <i>o</i> -F-Phe	T242G <i>Bs</i> DAAT ^a / <i>Pm</i> LAAD ^{a,65}	>99	>99
	H359Y <i>Av</i> PAL ^a / <i>Pmir</i> LAAD ^{a,90}	77	>99
	N347A <i>Av</i> PAL ^b / <i>Pmir</i> LAAD ^{b,91}	72	>99
D- <i>m</i> -F-Phe	T242G <i>Bs</i> DAAT ^a / <i>Pm</i> LAAD ^{a,65}	>99	99
	H359Y <i>Av</i> PAL ^a / <i>Pmir</i> LAAD ^{a,90}	74	98
	N347A <i>Av</i> PAL ^b / <i>Pmir</i> LAAD ^{b,91}	91	>99
	AncLAAO-N4 ^c / <i>catalase</i> / <i>Cg</i> DAADH/ <i>Bm</i> GDH ¹⁴²	(1.3 ^e)	>99
D- <i>p</i> -F-Phe	<i>Pmir</i> LAAD ^a / <i>Cg</i> DAADH ^a / <i>Bm</i> GDH ^{a,39}	(81 ^e)	>99
	T242G <i>Bs</i> DAAT ^a / <i>Pmir</i> LAAD ^{a,65}	>99	99
	H359Y <i>Av</i> PAL ^a / <i>Pmir</i> LAAD ^{a,90}	62	>99
	N347A <i>Av</i> PAL ^b / <i>Pmir</i> LAAD ^{b,91}	69	>99
	H359Y <i>Av</i> PAL ^a / <i>Pmir</i> LAAD ^{a,90}	78	>99
D-3,5-F ₂ -Phe	T242G <i>Bs</i> DAAT ^a / <i>Pmir</i> LAAD ^{a,65}	>99	>99
D- <i>p</i> -Br-Phe	T242G <i>Bs</i> DAAT ^a / <i>Pmir</i> LAAD ^{a,65}	>99	>99
	AncLAAO-N4 ^c / <i>catalase</i> / <i>Cg</i> DAADH/ <i>Bm</i> GDH ¹⁴²	(6.9 ^e)	>99
D- <i>m</i> -Cl-Phe	H359Y <i>Av</i> PAL ^a / <i>Pmir</i> LAAD ^{a,90}	63	99
D- <i>p</i> -Cl-Phe	T242G <i>Bs</i> DAAT ^a / <i>Pm</i> LAAD ^{a,65}	>99	>99
D- <i>o</i> -OH-Phe	N347A <i>Av</i> PAL ^b / <i>Pmir</i> LAAD ^{b,91}	26	72
(D- <i>p</i> -OH-Phe)	N347A <i>Av</i> PAL ^b / <i>Pmir</i> LAAD ^{b,91}	13	90
D-Tyr	<i>Bs</i> DAAT ^{b,f} / <i>St</i> DAPDH ^b / <i>Tb</i> ADH ^{b,149}	>99	>99
D- <i>o</i> -NO ₂ -Phe	H359Y <i>Av</i> PAL ^a / <i>Pmir</i> LAAD ^{a,90}	80	98
	N347A <i>Av</i> PAL ^b / <i>Pmir</i> LAAD ^{b,91}	78	>99
D- <i>m</i> -NO ₂ -Phe	H359Y <i>Av</i> PAL ^a / <i>Pmir</i> LAAD ^{a,90}	74	98
	N347A <i>Av</i> PAL ^b / <i>Pmir</i> LAAD ^{b,91}	96	>99
D- <i>p</i> -NO ₂ -Phe	H359Y <i>Av</i> PAL ^a / <i>Pmir</i> LAAD ^{a,90}	79	>99
	N347A <i>Av</i> PAL ^b / <i>Pmir</i> LAAD ^{b,91}	69	>99
D- <i>p</i> -CF ₃ -Phe	H359Y <i>Av</i> PAL ^a / <i>Pmir</i> LAAD ^{a,90}	64	98
D- <i>p</i> -CN-Phe	H359Y <i>Av</i> PAL ^a / <i>Pmir</i> LAAD ^{a,90}	77	99
D-3,4-OCH ₂ O-Phe	<i>Pmir</i> LAAD ^a / <i>Cg</i> DAADH ^a / <i>Bm</i> GDH ^{a,39}	(69 ^e)	98

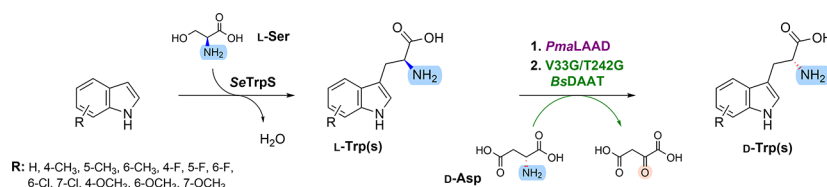
^aWhole-cell biocatalysts. ^bPurified enzyme. ^cCell-free multienzyme system. ^dProductivity (in g/L). ^eIsolation yield (%) at 100 mg scale. ^fProcedure considered asymmetric synthesis.

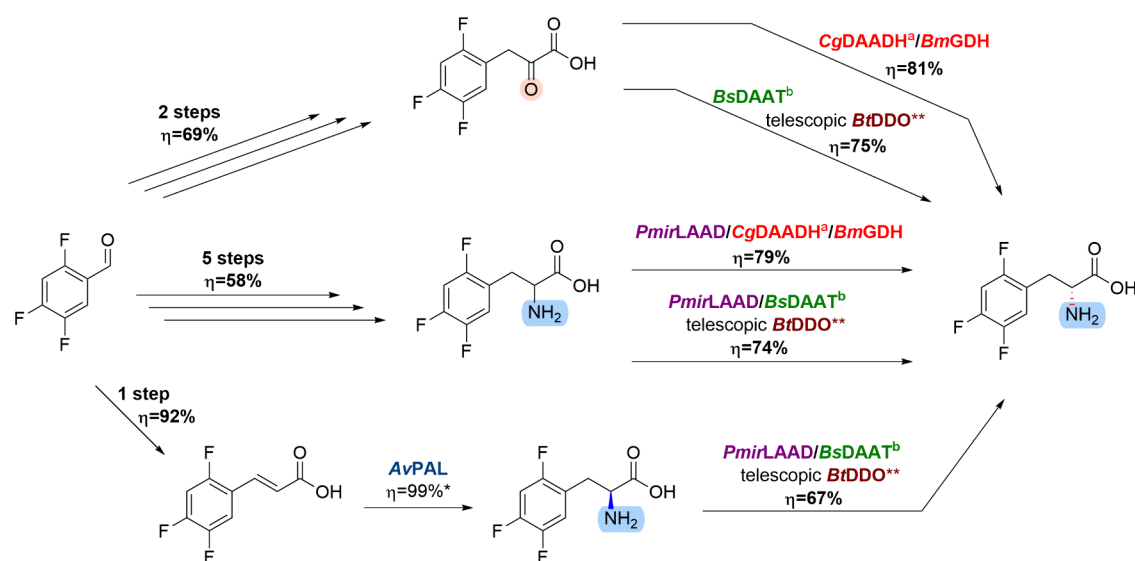
**Figure 26.** DAAT/DAADH/ADH cascade producing D-Phe and D-Tyr with high conversion (c) and an enantiomeric excess (ee) within a 9–12 h reaction time (R_T).¹⁴⁹**Figure 27.** PAL/LAAD cascade of cinnamic acids with electron-withdrawing ring substituents coupled with a chemical or enzymatic, DAAT- or DAADH-mediated, reduction.

substrate concentrations of 100 mM, achieving an overall yield of 43% and diminished waste values. When LAAD is omitted, in the case of the DAAT/DDO cascade, only 25 mM substrate concentration can be reached, but the number of steps is reduced to three. This resulted in an increased global yield of 52% and a reduced sEF from 41 to 30 of the five-step process (Table 8). The DAADH/GDH system provided a high yield of 56%, with mostly reduced waste and environmental factor (sEF of 21), compared to the 46% yield and sEF of 41 observed when coupled with the LAAD-mediated deracemization step within the LAAD/DAADH/GDH cascade. While each tested process has certain advantages and disadvantages, it is notable that the environmental footprints in all cases positioned well below the current procedures of obtaining D-phenylalanines, highlighting their enormous synthetic potential.¹⁵⁰

6. CONCLUSIONS AND OUTLOOK

The enzymatic synthesis of D-phenylalanines has emerged as an efficient and environmentally friendly approach for the production of these valuable chiral building blocks for

**Figure 25.** TrpS-mediated asymmetric synthesis coupled with the LAAD/DAAT cascade. Reproduced with permission from ref 147. Copyright 2019 American Chemical Society).



^aengineered CgDAADH (Q151L/D155G/T170I/R196M/H245N CgDAADH); ^b 242G BsDAAT; *in 4 M H₂NCOONH₄, pH 9.9; **additional product purification step with BtDDO

Figure 28. Chemoenzymatic routes using the readily available substituted benzaldehyde as starting material, optimized for the synthesis of D-2,3,5-trifluorophenylalanine. The three chemical routes consist of a different number of steps and lead with different global yields to the corresponding phenylpyruvate derivative to the racemic or L-phenylalanine analogue or to 2,3,5-trifluorocinnamate, which serves as a starting point for the diverse enzymatic cascades, each providing in high yields (67–81%) the sitagliptin intermediate, D-2,3,5-trifluorophenylalanine. Reproduced with permission from ref 150. Copyright 2019 Royal Society of Chemistry.

Table 8. Comparison of the Overall Yield, Number of Steps, Substrate Concentration, and E-Factor of the Chemoenzymatic Routes Leading to D-2,3,5-Trifluorophenylalanine^a

chemoenzymatic cascade		overall yield (%)	No. of steps	substrate loading (mM)	simplified E-factor
chemical steps	enzymatic steps				
Erlenmeyer–Plöchl synthesis	CgDAADH/BmGDH	56	3	50	21
	T242G BsDAAT/BtDDO	52	3	25	30
malonic ester synthesis	PmirLAAD/CgDAADH/BmGDH	46	6	50	41
	PmirLAAD/T242G BsDAAT/BtDDO	43	6	100	41
Knoevenagel–Doebner condensation	AvPAL/PmirLAAD/T242G BsDAAT/BtDDO	62	2	25	65

^aTable was reprinted with permission as a modified version from ref 150. Copyright 2019 Royal Society of Chemistry.

pharmaceuticals and fine chemicals. Biocatalysts, such as D-amino acid dehydrogenases (DAADHs) and D-amino acid transaminases (DAATs) enable the asymmetric synthesis of D-phenylalanines leveraging the prochiral phenylpyruvates as starting materials. Recent breakthroughs in protein engineering have considerably increased the activity, selectivity, and stability of these enzymes, broadening their applications. The directed evolution and rational design-based approaches have been pivotal in overcoming substrate scope limitations and substrate inhibition issues and for improving their catalytic efficiency for large-scale applications. The development of the first DAADH of broad substrate scope, achieved through rounds of error-prone PCR of *meso*-2,6-diamino-pimelic acid D-dehydrogenase (DAPDH) from *Corynebacterium glutamicum*,³³ paved the way for the development of DAADHs from DAPDHs of diverse sources. While the DAADH from *Ureibacillus thermosphaericus* (UtDAADH) shows increased thermostability and yields of D-Phe production,^{40,41} the DAADH from *Symbiobacterium thermophilum* (StDAADH) as a prototype of type II DAPDHs possess relaxed natural substrate specificity in the reductive amination route.^{49,51} Structure-guided engineering of several type II DAPDHs

provided highly effective variants for the reductive amination of various phenylpyruvate derivatives (Figure 12). DAADHs engineered from both type I and type II DAPDH classes showed high catalytic efficiencies in the reductive amination of phenylpyruvate, with the best performing variants exhibiting excellent turnover numbers (k_{cat}) ranging from 6 to 55 s^{−1} (Table 1). While several engineered variants have been employed for the preparative-scale reductive amination yielding D-Phe, their application for the production of substituted D-Phe analogues has been less studied, with the exception of CgDAADH.³⁹

For the reductive amination of phenylpyruvates by D-amino acid transaminases (DAATs), naturally occurring bacterial DAATs have been explored and engineered. Rational engineering of DAAT from *Bacillus* sp. YM-1, with broad amino donor and amino acceptor substrate specificity,⁶³ provided variants with enhanced activity toward various phenylpyruvic acids (Table 2),⁶⁵ approaching the activity of the wild-type DAAT for D-alanine.⁷⁶ Despite their broad substrate specificity, the applicability of DAATs has been limited by the unfavorable position of the reaction equilibrium toward the reduction amination. Accordingly, process engi-

neering efforts have been directed toward shifting the equilibrium to the desired direction, integrating the DAAT-mediated reaction in biosynthetic and/or enzymatic cascades.^{72–74}

As an attractive synthetic approach, the asymmetric hydroamination of cinnamic acids, catalyzed by phenylalanine ammonia-lyases (PALs), was also targeted for the synthesis of D-Phe. Albeit, reversing the natural L-selectivity of PALs remains a highly challenging engineering task. Saturation mutagenesis at 48 residues of AvPAL resulted in variants with increased D-selectivity, mostly for substrates with electron-withdrawing ring-substituents, but still no significant enrichment in the D-enantiomer as the product of the hydroamination reaction was obtained.⁹⁰ Nonetheless, by exploiting the non-stereoselective MIO-independent pathway, the efficient production of D-phenylalanines could be achieved by combining the H359Y AvPAL-catalyzed hydroamination with the L-amino acid deaminase (LAAD)-mediated oxidation of the undesired L-Phe in various enzyme cascades.^{90,91,150}

The build up of enzyme cascades are aimed to replace phenylpyruvates with the more accessible racemic or L-Phe as starting materials for the production of D-Phe. Within these cascades, the phenylpyruvate is provided *in situ* by an oxidation step catalyzed by either LAAD or L-amino acid oxidase (LAAO), followed by the DAADH and/or DAAT-mediated reductive amination.¹⁰¹ Protein engineering of LAADs or the development of ancestral LAAOs with high expression yield, and capable of transforming L-phenylalanines, have been crucial for the development of efficient cascades for the manufacture of D-phenylalanine derivatives (Tables 6 and 7). When compared in terms of productivity and environmental impact, certain advantages and disadvantages of the particular enzymatic processes have been identified, but their low-level environmental footprints highlight their enormous synthetic potential.¹⁵⁰

Considering the diversity of the biocatalyst toolbox available for the production of D-phenylalanines, future efforts should focus on protein engineering tasks aiming to fine-tune and tailor these biocatalysts toward a specifically targeted reaction, by increasing their turnover rates and operational stability and/or by alleviating substrate/product inhibition issues, to meet industrial requirements. In this context, the implementation and development of immobilization procedures, less explored for DAADHs,^{46,47} DAATs,¹⁵¹ and LAAOs^{152,153} are also desirable, allowing the setup of multienzymatic cascades in the form of continuous-flow processes. Such tailored biocatalytic toolboxes will contribute and enable facile and environmentally friendly access to D-phenylalanines, strengthening their position as highly valuable chiral building blocks.

AUTHOR INFORMATION

Corresponding Author

László Csaba Bencze – Enzymology and Applied Biocatalysis Research Center, Faculty of Chemistry and Chemical Engineering, Babeş-Bolyai University, RO-400028 Cluj-Napoca, Romania; orcid.org/0000-0003-0956-9749; Email: laszlo.bencze@ubbcluj.ro

Authors

Raluca Bianca Tomoiagă – Enzymology and Applied Biocatalysis Research Center, Faculty of Chemistry and Chemical Engineering, Babeş-Bolyai University, RO-400028 Cluj-Napoca, Romania

Levente Csaba Nagy – Enzymology and Applied Biocatalysis Research Center, Faculty of Chemistry and Chemical Engineering, Babeş-Bolyai University, RO-400028 Cluj-Napoca, Romania

Krisztina Boros – Enzymology and Applied Biocatalysis Research Center, Faculty of Chemistry and Chemical Engineering, Babeş-Bolyai University, RO-400028 Cluj-Napoca, Romania

Mădălina Elena Moisă – Enzymology and Applied Biocatalysis Research Center, Faculty of Chemistry and Chemical Engineering, Babeş-Bolyai University, RO-400028 Cluj-Napoca, Romania

Complete contact information is available at:
<https://pubs.acs.org/10.1021/acscatal.5c00837>

Author Contributions

L.C.B. conceived and wrote the manuscript with R.B.T., L.C.N., K.B., and M.E.M. All authors have given approval to the final version of the manuscript.

Notes

The authors declare no competing financial interest.

ACKNOWLEDGMENTS

This work was supported by the BACPROBIO Project funded by European Union – NextGenerationEU and the Romanian Government, under National Recovery and Resilience Plan for Romania, Contract No. 760251/28.12.2023, cod PNRR-C9-I8-CF92/31.07.2023, through the Romanian Ministry of Research, Innovation and Digitalization, within Component 9, Investment I8.

REFERENCES

- (1) Parmeggiani, F.; Weise, N. J.; Ahmed, S. T.; Turner, N. J. Synthetic and therapeutic applications of ammonia-lyases and aminomutases. *Chem. Rev.* **2018**, *118* (1), 73–118.
- (2) Kwa, A.; Kasiakou, S. K.; Tam, V. H.; Falagas, M. E. Polymyxin B: similarities to and differences from colistin (polymyxin E). *Expert Rev. Anti-infect. Ther.* **2007**, *5* (5), 811–821.
- (3) Solanas, C.; de la Torre, B. G.; Fernandez-Reyes, M.; Santiveri, C. M.; Jimenez, M. A.; Rivas, L.; Jimenez, A. I.; Andreu, D.; Cativiela, C. Therapeutic index of Gramicidin S is strongly modulated by D-phenylalanine analogues at the beta-turn. *J. Med. Chem.* **2009**, *52* (3), 664–674.
- (4) Chachin, M.; Yamada, M.; Fujita, A.; Matsuoka, T.; Matsushita, K.; Kurachi, Y. Nateglinide, a D-phenylalanine derivative lacking either a sulfonylurea or benzamido moiety, specifically inhibits pancreatic beta-cell-type K-ATP channels. *J. Pharmacol. Exp. Ther.* **2003**, *304* (3), 1025–1032.
- (5) Zashikhina, N.; Sharoyko, V.; Antipchik, M.; Tarasenko, I.; Anufrikov, Y.; Lavrentieva, A.; Tennikova, T.; Korzhikova-Vlakh, E. Novel formulations of C-peptide with long-acting therapeutic potential for treatment of diabetic complications. *Pharmaceutics* **2019**, *11* (1), 27.
- (6) Zhao, P.; Wang, J. Y.; Ma, H.; Xiao, Y.; He, L. L.; Tong, C.; Wang, Z. H.; Zheng, Q. S.; Dolence, E. K.; Nair, S.; et al. A newly synthetic chromium complex-Chromium (D-phenylalanine)(3) activates AMP-activated protein kinase and stimulates glucose transport. *Biochem. Pharmacol.* **2009**, *77* (6), 1002–1010.
- (7) Lenstra, D. C.; Damen, E.; Leenders, R. G. G.; Blaauw, R. H.; Rutjes, F.; Wegert, A.; Mecinovic, J. Structure-activity relationship studies on (R)-PFI-2 analogues as inhibitors of histone lysine methyltransferase SETD7. *ChemMedChem.* **2018**, *13* (14), 1405–1413.
- (8) Dong, L. M.; Marakovits, J.; Hou, X. J.; Guo, C. X.; Greasley, S.; Dagostino, E.; Ferre, R.; Johnson, M. C.; Kraynov, E.; Thomson, J.;

- et al. Structure-based design of novel human Pin1 inhibitors (II). *Bioorg. Med. Chem. Lett.* **2010**, 20 (7), 2210–2214.
- (9) Hwang, T. L.; Hung, C. H.; Hsu, C. Y.; Huang, Y. T.; Tsai, Y. C.; Hsieh, P. W. Design and synthesis of tryptophan containing dipeptide derivatives as formyl peptide receptor 1 antagonist. *Org. Biomol. Chem.* **2013**, 11 (22), 3742–3755.
- (10) Roques, B.; Anne, C.; Turcaud, S.; Fournie-Zaluski, M.-C. Type B botulinum toxin inhibitors. 2004/0176333 A1, 2004.
- (11) Yang, B.; Lamb, M. L.; Zhang, T.; Hennessy, E. J.; Grewal, G.; Sha, L.; Zambrowski, M.; Block, M. H.; Dowling, J. E.; Su, N.; et al. Discovery of Potent KIF1 Inhibitors Using a Method of Integrated High-Throughput Synthesis and Screening. *J. Med. Chem.* **2014**, 57 (23), 9958–9970.
- (12) Taniguchi, A.; Sasaki, D.; Shiohara, A.; Iwatsubo, T.; Tomita, T.; Sohma, Y.; Kanai, M. Attenuation of the aggregation and neurotoxicity of amyloid-beta peptides by catalytic photooxygenation. *Angew. Chem., Int. Ed.* **2014**, 53 (5), 1382–1385.
- (13) Saupé, S. M.; Leubner, S.; Betz, M.; Klebe, G.; Steinmetzer, T. Development of new cyclic plasmin inhibitors with excellent potency and selectivity. *J. Med. Chem.* **2013**, 56 (3), 820–831.
- (14) Tian, X.; Switzer, A. G.; Derosé, S. A.; Mishra, R. K.; Solinsky, M. G.; Mumin, R. N.; Ebetino, F. H.; Jayasinghe, L. R.; Webster, M. E.; Colson, A. O.; et al. Discovery of orally bioavailable 1,3,4-trisubstituted 2-oxopiperazine-based melanocortin-4 receptor agonists as potential antiobesity agents. *J. Med. Chem.* **2008**, 51 (19), 6055–6066.
- (15) Martínez-Rodríguez, S.; Torres, J. M.; Sánchez, P.; Ortega, E. Overview on multienzymatic cascades for the production of non-canonical α -amino acids. *Front. Bioeng. Biotechnol.* **2020**, 8, 887.
- (16) Xue, Y. P.; Cao, C. H.; Zheng, Y. G. Enzymatic asymmetric synthesis of chiral amino acids. *Chem. Soc. Rev.* **2018**, 47 (4), 1516–1561.
- (17) Gao, X. Z.; Ma, Q. Y.; Zhu, H. L. Distribution, industrial applications, and enzymatic synthesis of D-amino acids. *Appl. Microbiol. Biotechnol.* **2015**, 99 (8), 3341–3349.
- (18) Servi, S.; Tessaro, D.; Pedrocchi-Fantoni, G. Chemo-enzymatic deracemization methods for the preparation of enantiopure non-natural α -amino acids. *Coord. Chem. Rev.* **2008**, 252 (5–7), 715–726.
- (19) Pollegioni, L.; Rosini, E.; Molla, G. Advances in enzymatic synthesis of D-amino acids. *Int. J. Mol. Sci.* **2020**, 21 (9), 3206.
- (20) Schwarm, M. Application of whole-cell biocatalysts in the manufacture of fine chemicals. *Pharmaceutical Process Chemistry*; Wiley-VCH Verlag GmbH & Co., 2010; pp 183–205.
- (21) Bäter, A. J.; Venables, W. A. Characterization of inducible dehydrogenases specific for oxidation OF D-alanine, allohydroxy-D-proline, choline and sarcosine as peripheral membrane proteins in *Pseudomonas aeruginosa*. *Biochim. Biophys. Acta* **1977**, 468 (2), 209–226.
- (22) Marshall, V. P.; Sokatch, J. R. Oxidation of D-amino acids by a particulate enzyme from *Pseudomonas aeruginosa*. *J. Bacteriol.* **1968**, 95 (4), 1419–1424.
- (23) Tsukada, K. D-amino acid dehydrogenases of *Pseudomonas fluorescens*. *J. Biol. Chem.* **1966**, 241 (19), 4522–4528.
- (24) Satomura, T.; Kawakami, R.; Sakuraba, H.; Ohshima, T. Dye-linked D-proline dehydrogenase from hyperthermophilic archaeon *Pyrobaculum islandicum* is a novel FAD-dependent amino acid dehydrogenase. *J. Biol. Chem.* **2002**, 277 (15), 12861–12867.
- (25) Wild, J.; Walczak, W.; Krajewska-Grynkiewicz, K.; Ktopotowski, T. D-amino acid dehydrogenase: The enzyme of the first step of D-histidine and D-methionine racemization in *Salmonella typhimurium**. *Mol. Gen. Genet.* **1974**, 128 (2), 131–146.
- (26) Franklin, F. C. H.; Venables, W. A. Biochemical, genetic, and regulatory studies of alanine catabolism in *Escherichia coli* K12. *Mol. Gen. Genet.* **1976**, 149 (2), 229–237.
- (27) Raunio, R. P.; Jenkins, W. T. D-alanine oxidase form *Escherichia coli*: localization and induction by L-alanine. *J. Bacteriol.* **1973**, 115 (2), 560–566.
- (28) Raunio, R. P.; Straus, L. D.; Jenkins, W. T. D-alanine oxidase from *Escherichia coli*: participation in the oxidation of L-alanine. *J. Bacteriol.* **1973**, 115 (2), 567–573.
- (29) Cambon, E.; Piamtongkam, R.; Bordes, F.; Duquesne, S.; Andre, I.; Marty, A. Rationally engineered double substituted variants of *Yarrowia lipolytica* lipase with enhanced activity coupled with highly inverted enantioselectivity towards 2-bromo phenyl acetic acid esters. *Biotechnol. Bioeng.* **2010**, 106 (6), 852–859.
- (30) Boersma, Y. L.; Pijning, T.; Bosma, M. S.; van der Sloot, A. M.; Godinho, L. F.; Droge, M. J.; Winter, R. T.; van Pouderooyen, G.; Dijkstra, B. W.; Quax, W. J. Loop grafting of *Bacillus subtilis* lipase A: Inversion of enantioselectivity. *Chem. Biol.* **2008**, 15 (8), 782–789.
- (31) Hu, H. J.; Wang, Q. Q.; Wang, D. X.; Ao, Y. F. Modification of the enantioselectivity of biocatalytic meso-desymmetrization for synthesis of both enantiomers of cis-1,2-disubstituted cyclohexane by amidase engineering. *Adv. Synth. Catal.* **2021**, 363 (19), 4538–4543.
- (32) Li, A. P.; Wang, T.; Tian, Q.; Yang, X. H.; Yin, D. M.; Qin, Y.; Zhang, L. B. Single-point mutant inverts the stereoselectivity of a carbonyl reductase toward beta-ketoesters with enhanced activity. *Chem.–Eur. J.* **2021**, 27 (20), 6283–6294.
- (33) Vedha-Peters, K.; Gunawardana, M.; Rozzell, J. D.; Novick, S. J. Creation of a broad-range and highly stereoselective D-amino acid dehydrogenase for the one-step synthesis of D-amino acids. *J. Am. Chem. Soc.* **2006**, 128 (33), 10923–10929.
- (34) Scapin, G.; Cirilli, M.; Reddy, S. G.; Gao, Y.; Vederas, J. C.; Blanchard, J. S. Substrate and inhibitor binding sites in *Corynebacterium glutamicum* diaminopimelate dehydrogenase. *Biochemistry* **1998**, 37 (10), 3278–3285.
- (35) Schruppf, B.; Schwarzer, A.; Kalinowski, J.; Puhler, A.; Eggeling, L.; Sahm, H. A functionally split pathway for lysine synthesis in *Corynebacterium glutamicum*. *J. Bacteriol.* **1991**, 173 (14), 4510–4516.
- (36) Gao, X. Z.; Zhang, Z.; Zhang, Y.; Li, Y.; Zhu, H.; Wang, S.; Li, C. A newly determined member of the meso-diaminopimelate dehydrogenase family with a broad substrate spectrum. *Appl. Environ. Microbiol.* **2017**, 83 (11), No. e00476-17.
- (37) Reddy, S. G.; Scapin, G.; Blanchard, J. S. Expression, purification, and crystallization of meso-diaminopimelate dehydrogenase from *Corynebacterium glutamicum*. *Proteins: Struct. Funct. Genet.* **1996**, 25 (4), 514–516.
- (38) Cirilli, M.; Scapin, G.; Sutherland, A.; Vederas, J. C.; Blanchard, J. S. The three-dimensional structure of the ternary complex of *Corynebacterium glutamicum* diaminopimelate dehydrogenase-NADPH-L-2-amino-6-methylene-pimelate. *Protein Sci.* **2000**, 9 (10), 2034–2037.
- (39) Parmeggiani, F.; Ahmed, S. T.; Thompson, M. P.; Weise, N. J.; Galman, J. L.; Gahllo, D.; Dunstan, M. S.; Leys, D.; Turner, N. J. Single-biocatalyst synthesis of enantiopure D-arylalanines exploiting an engineered D-amino acid dehydrogenase. *Adv. Synth. Catal.* **2016**, 358 (20), 3298–3306.
- (40) Akita, H.; Fujino, Y.; Doi, K.; Ohshima, T. Highly stable meso-diaminopimelate dehydrogenase from an *Ureibacillus thermosphaericus* strain A1 isolated from a Japanese compost: purification, characterization and sequencing. *Amb. Express* **2011**, 1, 43.
- (41) Hayashi, J.; Seto, T.; Akita, H.; Watanabe, M.; Hoshino, T.; Yoneda, K.; Ohshima, T.; Sakuraba, H. Structure-based engineering of an artificially generated NADP(+)-dependent D-amino acid dehydrogenase. *Appl. Environ. Microbiol.* **2017**, 83 (11), No. e00491-17.
- (42) Liu, W. D.; Li, Z.; Huang, C. H.; Guo, R. T.; Zhao, L. M.; Zhang, D. L.; Chen, X.; Wu, Q. Q.; Zhu, D. M. Structural and mutational studies on the unusual substrate specificity of meso-diaminopimelate dehydrogenase from *Symbiobacterium thermophilum*. *ChemBioChem.* **2014**, 15 (2), 217–222.
- (43) Akita, H.; Suzuki, H.; Doi, K.; Ohshima, T. Efficient synthesis of D-branched-chain amino acids and their labeled compounds with stable isotopes using D-amino acid dehydrogenase. *Appl. Microbiol. Biotechnol.* **2014**, 98 (3), 1135–1143.

- (44) Akita, H.; Doi, K.; Kawarabayashi, Y.; Ohshima, T. Creation of a thermostable NADP⁺-dependent d-amino acid dehydrogenase from *Ureibacillus thermosphaericus* strain A1 meso-diaminopimelate dehydrogenase by site-directed mutagenesis. *Biotechnol. Lett.* **2012**, *34* (9), 1693–1699.
- (45) Ji, Z.; Zhang, Q.; Duan, L.; Dong, L.; Wang, S. Design of motifs interfacial interactions by co-evolved analysis of D-amino acid dehydrogenase for stability enhancement. *AIChE J.* **2023**, *69* (11), No. e18214.
- (46) Boros, K.; Gal, L.; Gal, C. A.; Wäscher, M.; Tomoiaga, R. B.; Tosa, M. I.; Pietruszka, J.; Bencze, L. C. Immobilization of D-amino acid dehydrogenase from *Ureibacillus thermosphaericus*. *Process Biochem.* **2024**, *140*, 45–55.
- (47) Lei, H. B.; Zhang, Q.; Xiang, X. Y.; Jiang, L.; Wang, S. Y.; Duan, L. X.; Wang, S. Z. Metal-organic framework hybrid materials of ZIF-8/RGO for immobilization of D-amino acid dehydrogenase. *Nano Res.* **2024**, *17* (1), 290–296.
- (48) Liu, W. D.; Guo, R. T.; Chen, X.; Li, Z.; Gao, X. Z.; Huang, C. H.; Wu, Q. Q.; Feng, J. H.; Zhu, D. M. Structural analysis reveals the substrate-binding mechanism for the expanded substrate specificity of mutant meso-diaminopimelate dehydrogenase. *ChemBioChem.* **2015**, *16* (6), 924–929.
- (49) Gao, X. Z.; Chen, X.; Liu, W. D.; Feng, J. H.; Wu, Q. Q.; Hua, L.; Zhu, D. M. A novel meso-diaminopimelate dehydrogenase from *Symbiobacterium thermophilum*: Overexpression, characterization, and potential for D-amino acid synthesis. *Appl. Environ. Microbiol.* **2012**, *78* (24), 8595–8600.
- (50) Zhang, Y. N.; Ma, Q. Y.; Dong, M. M.; Zhang, X. H.; Chen, Y. C.; Gao, X. Z.; Song, Y. D. Essential role of amino acid position 71 in substrate preference by meso-diaminopimelate dehydrogenase from *Symbiobacterium thermophilum* IAM14863. *Enzyme Microb. Technol.* **2018**, *111*, 57–62.
- (51) Gao, X. Z.; Huang, F.; Feng, J. H.; Chen, X.; Zhang, H. L.; Wang, Z. X.; Wu, Q. Q.; Zhu, D. M. Engineering the meso-diaminopimelate dehydrogenase from *Symbiobacterium thermophilum* by site saturation mutagenesis for D-phenylalanine synthesis. *Appl. Environ. Microbiol.* **2013**, *79* (16), 5078–5081.
- (52) Cheng, X. K.; Chen, X.; Feng, J. H.; Wu, Q. Q.; Zhu, D. M. Structure-guided engineering of meso-diaminopimelate dehydrogenase for enantioselective reductive amination of sterically bulky 2-keto acids. *Catal. Sci. Technol.* **2018**, *8* (19), 4994–5002.
- (53) Lu, C.; Zhang, S.; Song, W.; Liu, J.; Chen, X. L.; Liu, L. M.; Wu, J. Efficient synthesis of D-phenylalanine from L-phenylalanine via a tri-enzymatic cascade pathway. *ChemCatChem.* **2021**, *13* (13), 3165–3173.
- (54) Wu, T. F.; Chen, Y. H.; Wei, W. Q.; Song, W.; Wu, J.; Wen, J.; Hu, G. P.; Li, X. M.; Gao, C.; Chen, X. L.; et al. Mechanism-guided computational design drives meso-diaminopimelate dehydrogenase to efficient synthesis of aromatic D-amino acids. *ACS Synth. Biol.* **2024**, *13* (6), 1879–1892.
- (55) Wei, Y.; Geng, Q.; Liu, H. P.; Wang, Y. Q.; Zhang, G. F.; Qian, X. L.; Yu, H. L.; Xu, J. H.; Zhang, Z. J. Hierarchical engineering of meso-diaminopimelate dehydrogenase for efficient synthesis of bulky D-amino acids. *ACS Catal.* **2024**, *14* (15), 11447–11456.
- (56) Gao, X. Z.; Ma, Q. Y.; Song, H. H.; Sun, X. M.; Li, Z. Y.; Liu, M. F. Altered cofactor preference of thermostable StDAPDH by a single mutation at K159. *Int. J. Mol. Sci.* **2020**, *21* (5), 1788.
- (57) Akita, H.; Nakamichi, Y.; Morita, T.; Matsushika, A. Identification and functional characterization of NAD(P)(+)-dependent meso-diaminopimelate dehydrogenase from *Numidum massiliense*. *MicrobiologyOpen* **2020**, *9* (8), No. e1059.
- (58) Akita, H.; Nakamichi, Y.; Morita, T.; Matsushika, A. Characterization of an NAD(P)(+)-dependent meso-diaminopimelate dehydrogenase from *Thermosyntropha lipolytica*. *Biochim. Biophys. Acta-Proteins Proteom.* **2020**, *1868* (10), 140476.
- (59) Thorne, C. B.; Gomez, C. G.; Housewright, R. D. Transamination of D-amino acids by *Bacillus subtilis*. *J. Bacteriol.* **1955**, *69* (3), 357–362.
- (60) Thorne, C. B.; Molnar, D. M. D-Amino acid transamination in *Bacillus anthracis*. *J. Bacteriol.* **1955**, *70* (4), 420–426.
- (61) Meadow, P.; Work, E. Bacterial transamination of the stereoisomers of diaminopimelic acid and lysine. *Biochim. Biophys. Acta* **1958**, *28* (C), 596–599.
- (62) Hug, D. H.; Werkman, C. H. Transamination in *Rhodospirillum rubrum*. *Arch. Biochem. Biophys.* **1957**, *72* (2), 369–375.
- (63) Yonaha, K.; Misono, H.; Yamamoto, T.; Soda, K. D-Amino acid aminotransferase of *Bacillus sphaericus*. Enzymologic and spectrometric properties. *J. Biol. Chem.* **1975**, *250* (17), 6983–6989.
- (64) Bae, H. S.; Hong, S. P.; Lee, S. G.; Kwak, M. S.; Esaki, N.; Sung, M. H. Application of a thermostable glutamate racemase from *Bacillus* sp SK-1 for the production of D-phenylalanine in a multi-enzyme system. *J. Mol. Catal. B Enzym.* **2002**, *17* (6), 223–233.
- (65) Walton, C. J. W.; Parmeggiani, F.; Barber, J. E. B.; McCann, J. L.; Turner, N. J.; Chica, R. A. Engineered aminotransferase for the production of D-phenylalanine derivatives using biocatalytic cascades. *ChemCatChem.* **2018**, *10* (2), 470–474.
- (66) Hohne, M.; Kuhl, S.; Robins, K.; Bornscheuer, U. T. Efficient asymmetric synthesis of chiral amines by combining transaminase and pyruvate decarboxylase. *ChemBioChem* **2008**, *9* (3), 363–365.
- (67) Pucci, M. J.; Thanassi, J. A.; Ho, H. T.; Falk, P. J.; Dougherty, T. J. *Staphylococcus haemolyticus* contains 2 D-glutamic acid biosynthetic activities, a glutamate racemase and a D-amino-acid transaminase. *J. Bacteriol.* **1995**, *177* (2), 336–342.
- (68) Taylor, P. P.; Fotheringham, I. G. Nucleotide sequence of the *Bacillus licheniformis* ATCC 10716 *dat* gene and comparison of the predicted amino acid sequence with those of other bacterial species. *Biochim. Biophys. Acta-Gene Struct. Expression* **1997**, *1350* (1), 38–40.
- (69) Fotheringham, I. G.; Bledig, S. A.; Taylor, P. P. Characterization of the genes encoding D-amino acid transaminase and glutamate racemase, two D-glutamate biosynthetic enzymes of *Bacillus sphaericus* ATCC 10208. *J. Bacteriol.* **1998**, *180* (16), 4319–4323.
- (70) Fotheringham, I. G.; Taylor, P. P.; Ton, J. L. Preparation of D-amino acids by direct fermentative means. U.S. patent US5728555A, 1998.
- (71) Kobayashi, J.; Shimizu, Y.; Mutaguchi, Y.; Doi, K.; Ohshima, T. Characterization of D-amino acid aminotransferase from *Lactobacillus salivarius*. *J. Mol. Catal. B Enzym.* **2013**, *94*, 15–22.
- (72) Park, E. S.; Dong, J. Y.; Shin, J. S. Biocatalytic asymmetric synthesis of unnatural amino acids through the cascade transfer of amino groups from primary amines onto keto acids. *ChemCatChem.* **2013**, *5* (12), 3538–3542.
- (73) Savile, C. K.; Janey, J. M.; Mundorff, E. C.; Moore, J. C.; Tam, S.; Jarvis, W. R.; Colbeck, J. C.; Krebber, A.; Fleitz, F. J.; Brands, J.; et al. Biocatalytic asymmetric synthesis of chiral amines from ketones applied to sitagliptin manufacture. *Science* **2010**, *329* (5989), 305–309.
- (74) Liu, R. X.; Liu, S. P.; Cheng, S.; Zhang, L.; Ding, Z. Y.; Gu, Z. H.; Shi, G. Y. Screening, characterization and utilization of D-amino acid aminotransferase to obtain D-phenylalanine. *Appl. Biochem. Microbiol.* **2015**, *51* (6), 695–703.
- (75) Fuchikami, Y.; Yoshimura, T.; Gutierrez, A.; Soda, K.; Esaki, N. Construction and properties of a fragmentary D-amino acid aminotransferase. *J. Biochem.* **1998**, *124* (5), 905–910.
- (76) Barber, J. E. B.; Damry, A. M.; Calderini, G. F.; Walton, C. J. W.; Chica, R. A. Continuous colorimetric screening assay for detection of D-amino acid aminotransferase mutants displaying altered substrate specificity. *Anal. Biochem.* **2014**, *463*, 23–30.
- (77) Peisach, D.; Chipman, D. M.; Van Ophem, P. W.; Manning, J. M.; Ringe, D. Crystallographic study of steps along the reaction pathway of D-amino acid aminotransferase. *Biochemistry* **1998**, *37* (14), 4958–4967.
- (78) Gloge, A.; Zon, J.; Kövári, A.; Poppe, L.; Rétey, J. Phenylalanine ammonia-lyase: The use of its broad substrate specificity for mechanistic investigations and biocatalysis - Synthesis of L-arylalanines. *Chem.-Eur. J.* **2000**, *6* (18), 3386–3390.
- (79) Filip, A.; Nagy, E. Z. A.; Tork, S. D.; Bánóczy, G.; Tosa, M. I.; Irimie, F. D.; Poppe, L.; Paizs, C.; Bencze, L. C. Tailored mutants of

- phenylalanine ammonia-lyase from *Petroselinum crispum* for the synthesis of bulky L- and D-arylalanines. *ChemCatChem*. **2018**, *10* (12), 2627–2633.
- (80) Tork, S. D.; Nagy, E. Z. A.; Cserepes, L.; Bordea, D. M.; Nagy, B.; Tosa, M. I.; Paizs, C.; Bencze, L. C. The production of L- and D-phenylalanines using engineered phenylalanine ammonia lyases from *Petroselinum crispum*. *Sci. Rep.* **2019**, *9*, 20123.
- (81) de Lange, B.; Hyett, D. J.; Maas, P. J. D.; Mink, D.; van Assema, F. B. J.; Sereinig, N.; de Vries, A. H. M.; de Vries, J. G. Asymmetric synthesis of (S)-2-indolinecarboxylic acid by combining biocatalysis and homogeneous catalysis. *ChemCatChem*. **2011**, *3* (2), 289–292.
- (82) Hardegger, L. A.; Beney, P.; Bixel, D.; Fleury, C.; Gao, F.; Perrenoud, A. G. G.; Gu, X. X.; Haber, J.; Hong, T.; Humair, R.; et al. Toward a scalable synthesis and process for EMA401, Part III: Using an engineered phenylalanine ammonia lyase enzyme to synthesize a non-natural phenylalanine derivative. *Org. Process Res. Dev.* **2020**, *24* (9), 1763–1771.
- (83) Rowles, I.; Groenendaal, B.; Binay, B.; Malone, K. J.; Willies, S. C.; Turner, N. J. Engineering of phenylalanine ammonia lyase from *Rhodotorula glutinis* for the enhanced synthesis of unnatural L-amino acids. *Tetrahedron* **2016**, *72* (46), 7343–7347.
- (84) Bencze, L. C.; Filip, A.; Bánóczy, G.; Tosa, M. I.; Irimie, F. D.; Gellért, A.; Poppe, L.; Paizs, C. Expanding the substrate scope of phenylalanine ammonia-lyase from *Petroselinum crispum* towards styrylalanines. *Org. Biomol. Chem.* **2017**, *15* (17), 3717–3727.
- (85) Ahmed, S. T.; Parmeggiani, F.; Weise, N. J.; Flitsch, S. L.; Turner, N. J. Engineered ammonia lyases for the production of challenging electron-rich L-phenylalanines. *ACS Catal.* **2018**, *8* (4), 3129–3132.
- (86) Bartsch, S.; Bornscheuer, U. T. Mutational analysis of phenylalanine ammonia lyase to improve reactions rates for various substrates. *Protein Eng. Des. Sel.* **2010**, *23* (12), 929–933.
- (87) Nagy, E. Z. A.; Tork, S. D.; Lang, P. A.; Filip, A.; Irimie, F. D.; Poppe, L.; Tosa, M. I.; Schofield, C. J.; Brem, J.; Paizs, C.; et al. Mapping the hydrophobic substrate binding site of phenylalanine ammonia-lyase from *Petroselinum crispum*. *ACS Catal.* **2019**, *9* (9), 8825–8834.
- (88) Tomoiaga, R. B.; Tork, S. D.; Horváth, I.; Filip, A.; Nagy, L. C.; Bencze, L. C. Saturation mutagenesis for phenylalanine ammonia lyases of enhanced catalytic properties. *Biomolecules* **2020**, *10* (6), 838.
- (89) Sun, C. H.; Lu, G.; Chen, B. M.; Li, G. J.; Wu, Y.; Brack, Y.; Yi, D.; Ao, Y. F.; Wu, S. K.; Wei, R.; et al. Direct asymmetric synthesis of β -branched aromatic α -amino acids using engineered phenylalanine ammonia lyases. *Nat. Commun.* **2024**, *15* (1), 8264.
- (90) Parmeggiani, F.; Lovelock, S. L.; Weise, N. J.; Ahmed, S. T.; Turner, N. J. Synthesis of D- and L-Phenylalanine derivatives by phenylalanine ammonia lyases: A multienzymatic cascade process. *Angew. Chem., Int. Ed.* **2015**, *54* (15), 4608–4611.
- (91) Zhu, L. B.; Feng, G. Q.; Ge, F.; Song, P.; Wang, T. T.; Liu, Y.; Tao, Y. G.; Zhou, Z. M. One-pot enzymatic synthesis of D-arylalanines using phenylalanine ammonia lyase and L-amino acid deaminase. *Appl. Biochem. Biotechnol.* **2019**, *187* (1), 75–89.
- (92) Lovelock, S. L.; Lloyd, R. C.; Turner, N. J. Phenylalanine ammonia lyase catalyzed synthesis of amino acids by an MIO-cofactor independent pathway. *Angew. Chem., Int. Ed.* **2014**, *53* (18), 4652–4656.
- (93) Schuster, B.; Reteý, J. The mechanism of action of phenylalanine ammonia-lyase - The role of prosthetic dehydroalanine. *Proc. Natl. Acad. Sci. U. S. A.* **1995**, *92* (18), 8433–8437.
- (94) Pilbák, S.; Farkas, Ö.; Poppe, L. Mechanism of the tyrosine ammonia lyase reaction-Tandem nucleophilic and electrophilic enhancement by a proton transfer. *Chem.-Eur. J.* **2012**, *18* (25), 7793–7802.
- (95) Wybenga, G. G.; Szymanski, W.; Wu, B.; Feringa, B. L.; Janssen, D. B.; Dijkstra, B. W. Structural investigations into the stereochemistry and activity of a phenylalanine-2,3-aminomutase from *Taxus chinensis*. *Biochemistry* **2014**, *53* (19), 3187–3198.
- (96) Ratnayake, N. D.; Wanninayake, U.; Geiger, J. H.; Walker, K. D. Stereochemistry and mechanism of a microbial phenylalanine aminomutase. *J. Am. Chem. Soc.* **2011**, *133* (22), 8531–8533.
- (97) Feng, L.; Wanninayake, U.; Strom, S.; Geiger, J.; Walker, K. D. Mechanistic, mutational, and structural evaluation of a *Taxus* phenylalanine aminomutase. *Biochemistry* **2011**, *50* (14), 2919–2930.
- (98) Weise, N. J.; Ahmed, S. T.; Parmeggiani, F.; Galman, J. L.; Dunstan, M. S.; Charnock, S. J.; Leys, D.; Turner, N. J. Zymophore identification enables the discovery of novel phenylalanine ammonia lyase enzymes. *Sci. Rep.* **2017**, *7*, 13691.
- (99) Sciacovelli, O.; Dell'Atti, A.; De Giglio, A.; Cassidei, L. Studies on phenylpyruvic acid. *Z. Naturforsch. C* **1976**, *31* (1–2), 5–11.
- (100) Cooper, A. J.; Ginos, J. Z.; Meister, A. Synthesis and properties of the α -keto acids. *Chem. Rev.* **1983**, *83* (3), 321–358.
- (101) Leuchtenberger, W.; Huthmacher, K.; Drauz, K. Biotechnological production of amino acids and derivatives: current status and prospects. *Appl. Microbiol. Biotechnol.* **2005**, *69* (1), 1–8.
- (102) Pirrung, M. C.; Krishnamurthy, N. Preparation of (R)-phenylalanine analogs by enantioselective destruction using L-amino acid oxidase. *J. Org. Chem.* **1993**, *58* (4), 957–958.
- (103) Alexandre, F. R.; Pantaleone, D. P.; Taylor, P. P.; Fotheringham, I. G.; Ager, D. J.; Turner, N. J. Amine-boranes: effective reducing agents for the deracemisation of DL-amino acids using L-amino acid oxidase from *Proteus myxofaciens*. *Tetrahedron Lett.* **2002**, *43* (4), 707–710.
- (104) Molla, G.; Melis, R.; Pollegioni, L. Breaking the mirror: L-Amino acid deaminase, a novel stereoselective biocatalyst. *Biotechnol. Adv.* **2017**, *35* (6), 657–668.
- (105) Baek, J. O.; Seo, J. W.; Kwon, O.; Seong, S. I.; Kim, I. H.; Kim, C. H. Expression and characterization of a second L-amino acid deaminase isolated from *Proteus mirabilis* in *Escherichia coli*. *J. Basic Microbiol.* **2011**, *51* (2), 129–135.
- (106) Wu, L. C.; Guo, X. L.; Wu, G. B.; Liu, P. F.; Liu, Z. D. Efficient enzymatic synthesis of α -keto acids by redesigned substrate-binding pocket of the L-amino acid deaminase (*PmiLAAD*). *Enzyme Microb. Technol.* **2020**, *132*, 109393.
- (107) Liu, L.; Hossain, G. S.; Shin, H. D.; Li, J. H.; Du, G. C.; Chen, J. One-step production of α -ketoglutaric acid from glutamic acid with an engineered L-amino acid deaminase from *Proteus mirabilis*. *J. Biotechnol.* **2013**, *164* (1), 97–104.
- (108) Ju, Y. C.; Tong, S. L.; Gao, Y. X.; Zhao, W.; Liu, Q.; Gu, Q.; Xu, J.; Niu, L. W.; Teng, M. K.; Zhou, H. H. Crystal structure of a membrane-bound L-amino acid deaminase from *Proteus vulgaris*. *J. Struct. Biol.* **2016**, *195* (3), 306–315.
- (109) Hou, Y.; Hossain, G. S.; Li, J. H.; Shin, H. D.; Liu, L.; Du, G. C. Production of phenylpyruvic acid from L-phenylalanine using an L-amino acid deaminase from *Proteus mirabilis*: Comparison of enzymatic and whole-cell biotransformation approaches. *Appl. Microbiol. Biotechnol.* **2015**, *99* (20), 8391–8402.
- (110) Motta, P.; Molla, G.; Pollegioni, L.; Nardini, M. Structure-function relationships in L-amino acid deaminase, a flavoprotein belonging to a novel class of biotechnologically relevant enzymes. *J. Biol. Chem.* **2016**, *291* (20), 10457–10475.
- (111) Zhang, D. P.; Jing, X. R.; Fan, A. W.; Liu, H.; Nie, Y.; Xu, Y. Active expression of membrane-bound L-amino acid deaminase from *Proteus mirabilis* in recombinant *Escherichia coli* by fusion with maltose-binding protein for enhanced catalytic performance. *Catalysts* **2020**, *10* (2), 215.
- (112) Liu, J.; Liu, J. M.; Yang, B.; Gao, C.; Song, W.; Hu, G. P.; Liu, L. M.; Wu, J. Production of phenylpyruvic acid by engineered L-amino acid deaminase from *Proteus mirabilis*. *Biotechnol. Lett.* **2022**, *44* (5–6), 635–642.
- (113) Hou, Y.; Hossain, G. S.; Li, J. H.; Shin, H. D.; Du, G. C.; Liu, L. Combination of phenylpyruvic acid (PPA) pathway engineering and molecular engineering of L-amino acid deaminase improves PPA production with an *Escherichia coli* whole-cell biocatalyst. *Appl. Microbiol. Biotechnol.* **2016**, *100* (5), 2183–2191.
- (114) Hou, Y.; Hossain, G. S.; Li, J. H.; Shin, H. D.; Du, G. C.; Chen, J.; Liu, L. Metabolic engineering of cofactor flavin adenine

dinucleotide (FAD) synthesis and regeneration in *Escherichia coli* for production of α -keto acids. *Biotechnol. Bioeng.* **2017**, 114 (9), 1928–1936.

(115) Wu, Y. Y.; Zhang, S.; Song, W.; Liu, J.; Chen, X. L.; Hu, G. P.; Zhou, Y. W.; Liu, L. M.; Wu, J. Enhanced catalytic efficiency of L-amino acid deaminase achieved by a shorter hydride transfer distance. *ChemCatChem*. **2021**, 13 (21), 4557–4566.

(116) Fan, A. W.; Wang, Z. Y.; Qu, H. J.; Nie, Y.; Xu, Y. Semi-rational design of *Proteus mirabilis* L-amino acid deaminase for expanding its substrate specificity in α -keto acid synthesis from L-amino acids. *Catalysts* **2022**, 12 (2), 175.

(117) Motta, P.; Pollegioni, L.; Molla, G. Properties of L-amino acid deaminase: En route to optimize bioconversion reactions. *Biochimie* **2019**, 158, 199–207.

(118) Rosini, E.; Melis, R.; Molla, G.; Tessaro, D.; Pollegioni, L. Deracemization and stereoinversion of α -amino acids by L-amino acid deaminase. *Adv. Synth. Catal.* **2017**, 359 (21), 3773–3781.

(119) Melis, R.; Rosini, E.; Pirillo, V.; Pollegioni, L.; Molla, G. *In vitro* evolution of an L-amino acid deaminase active on L-1-naphthylalanine. *Catal. Sci. Technol.* **2018**, 8 (20), 5359–5367.

(120) Hossain, G. S.; Li, J. H.; Shin, H. D.; Du, G. C.; Liu, L.; Chen, J. L-Amino acid oxidases from microbial sources: Types, properties, functions, and applications. *Appl. Microbiol. Biotechnol.* **2014**, 98 (4), 1507–1515.

(121) Pollegioni, L.; Motta, P.; Molla, G. L-Amino acid oxidase as biocatalyst: A dream too far? *Appl. Microbiol. Biotechnol.* **2013**, 97 (21), 9323–9341.

(122) Geueke, B.; Hummel, W. Heterologous expression of *Rhodococcus opacus* L-amino acid oxidase in *Streptomyces lividans*. *Protein Expr. Purif.* **2003**, 28 (2), 303–309.

(123) Nuutinen, J. T.; Marttinen, E.; Soliymani, R.; Hildén, K.; Timonen, S. L-Amino acid oxidase of the fungus *Hebeloma cylindrosporum* displays substrate preference towards glutamate. *Microbiol.-SGM* **2012**, 158, 272–283.

(124) Bifulco, D.; Pollegioni, L.; Tessaro, D.; Servi, S.; Molla, G. A thermostable L-aspartate oxidase: a new tool for biotechnological applications. *Appl. Microbiol. Biotechnol.* **2013**, 97 (16), 7285–7295.

(125) Cheng, C. H.; Yang, C. A.; Liu, S. Y.; Lo, C. T.; Huang, H. C.; Liao, F. C.; Peng, K. C. Cloning of a novel L-amino acid oxidase from *Trichoderma harzianum* ETS 323 and bioactivity analysis of overexpressed L-amino acid oxidase. *J. Agric. Food Chem.* **2011**, 59 (17), 9142–9149.

(126) Tong, H. C.; Chen, W.; Shi, W. Y.; Qi, F. X.; Dong, X. Z. SO-LAAO, a novel L-amino acid oxidase that enables *Streptococcus oligofermentans* to outcompete *Streptococcus mutans* by generating H_2O_2 from peptone. *J. Bacteriol.* **2008**, 190 (13), 4716–4721.

(127) Hahn, K.; Neumeister, K.; Mix, A.; Kottke, T.; Groger, H.; Fischer von Mollard, G. Recombinant expression and characterization of a L-amino acid oxidase from the fungus *Rhizoctonia solani*. *Appl. Microbiol. Biotechnol.* **2017**, 101 (7), 2853–2864.

(128) Nakahara, A.; Su, Z. Y.; Wakayama, M.; Nakamura, M.; Sakakibara, K.; Matsui, D. Improvement of heterologous soluble expression of L-amino acid oxidase using logistic regression. *ChemBioChem* **2024**, 25 (13), No. e202400243.

(129) Bloess, S.; Beuel, T.; Kruger, T.; Sewald, N.; Dierks, T.; Fischer von Mollard, G. Expression, characterization, and site-specific covalent immobilization of an L-amino acid oxidase from the fungus *Hebeloma cylindrosporum*. *Appl. Microbiol. Biotechnol.* **2019**, 103 (5), 2229–2241.

(130) Hess, M. C.; Bloess, S.; Risse, J. M.; Friehs, K.; Fischer von Mollard, G. Recombinant expression of an L-amino acid oxidase from the fungus *Hebeloma cylindrosporum* in *Pichia pastoris* including fermentation. *MicrobiologyOpen* **2020**, 9 (10), No. e1112.

(131) Koopmeiners, S.; Gilzer, D.; Widmann, C.; Berelsmann, N.; Sproß, J.; Niemann, H. H.; Fischer von Mollard, G. Crystal structure and enzyme engineering of the broad substrate spectrum L-amino acid oxidase 4 from the fungus *Hebeloma cylindrosporum*. *FEBS Lett.* **2024**, 598 (18), 2306–2320.

(132) Nakano, S.; Minamino, Y.; Hasebe, F.; Ito, S. Deracemization and stereoinversion to aromatic D-amino acid derivatives with ancestral L-amino acid oxidase. *ACS Catal.* **2019**, 9 (11), 10152–10158.

(133) Tomoiaga, R. B.; Ursu, M.; Boros, K.; Nagy, L. C.; Bencze, L. C. Ancestral L-amino acid oxidase: From substrate scope exploration to phenylalanine ammonia-lyase assay. *J. Biotechnol.* **2023**, 377, 43–52.

(134) Nakano, S.; Kozuka, K.; Minamino, Y.; Karasuda, H.; Hasebe, F.; Ito, S. Ancestral L-amino acid oxidases for deracemization and stereoinversion of amino acids. *Commun. Chem.* **2020**, 3 (1), 181.

(135) Ishida, C.; Miyata, R.; Hasebe, F.; Miyata, A.; Kumazawa, S.; Ito, S.; Nakano, S. Reconstruction of hyper-thermostable ancestral L-amino acid oxidase to perform deracemization to D-amino acids. *ChemCatChem*. **2021**, 13 (24), 5228–5235.

(136) Kawamura, Y.; Ishida, C.; Miyata, R.; Miyata, A.; Hayashi, S.; Fujinami, D.; Ito, S.; Nakano, S. Structural and functional analysis of hyper-thermostable ancestral L-amino acid oxidase that can convert Trp derivatives to D-forms by chemoenzymatic reaction. *Commun. Chem.* **2023**, 6 (1), 200.

(137) Wu, Y. Y.; Cui, Y. Z.; Song, W.; Wei, W. Q.; He, Z. Z.; Tao, J. Y.; Yin, D. J.; Chen, X. L.; Gao, C.; Liu, J.; et al. Reprogramming the transition states to enhance C–N cleavage efficiency of *Rhodococcus opacus* L-amino acid oxidase. *JACS Au* **2024**, 4 (2), 557–569.

(138) Geueke, B.; Hummel, W. A new bacterial L-amino acid oxidase with a broad substrate specificity: purification and characterization. *Enzyme Microb. Technol.* **2002**, 31 (1–2), 77–87.

(139) Faust, A.; Niefind, K.; Hummel, W.; Schomburg, D. The structure of a bacterial L-amino acid oxidase from *Rhodococcus opacus* gives new evidence for the hydride mechanism for dehydrogenation. *J. Mol. Biol.* **2007**, 367 (1), 234–248.

(140) Zhang, D. P.; Jing, X. R.; Zhang, W. L.; Nie, Y.; Xu, Y. Highly selective synthesis of D-amino acids from readily available L-amino acids by a one-pot biocatalytic stereoinversion cascade. *RSC Adv.* **2019**, 9 (51), 29927–29935.

(141) Zhang, D. P.; Jing, X. R.; Wu, L. J.; Fan, A. W.; Nie, Y.; Xu, Y. Highly selective synthesis of D-amino acids via stereoinversion of corresponding counterpart by an in vivo cascade cell factory. *Microb. Cell Fact.* **2021**, 20 (1), 11.

(142) Araseki, H.; Sugishima, N.; Chisuga, T.; Nakano, S. Development of an enzyme cascade system for the synthesis of enantiomerically pure D-amino acids utilizing ancestral L-amino acid oxidase. *ChemBioChem*. **2024**, 25 (8), No. e202400036.

(143) Liese, A.; Seelbach, K.; Wandrey, C. Industrial biotransformations. Wiley-VCH: 2006.

(144) Taylor, P. P.; Pantaleone, D. P.; Senkpeil, R. F.; Fotheringham, I. G. Novel biosynthetic approaches to the production of unnatural amino acids using transaminases. *Trends Biotechnol.* **1998**, 16 (10), 412–418.

(145) Taylor, P. P.; Grinter, N. J.; McCarthy, S. L.; Pantaleone, D. P.; Ton, J. L.; Yoshida, R. K.; Fotheringham, I. G. D-phenylalanine biosynthesis using *Escherichia coli*: Creation of a new metabolic pathway. *ACS Symp. Ser.* **2001**, 776, 65–75.

(146) Bae, H. S.; Lee, S. G.; Hong, S. P.; Kwak, M. S.; Esaki, N.; Soda, K.; Sung, M. H. Production of aromatic D-amino acids from α -keto acids and ammonia by coupling of four enzyme reactions. *J. Mol. Catal. B Enzym.* **1999**, 6 (3), 241–247.

(147) Parmeggiani, F.; Casamajo, A. R.; Walton, C. J. W.; Galman, J. L.; Turner, N. J.; Chica, R. A. One-pot biocatalytic synthesis of substituted D-tryptophans from indoles enabled by an engineered aminotransferase. *ACS Catal.* **2019**, 9 (4), 3482–3486.

(148) Almhjell, P. J.; Johnston, K. E.; Porter, N. J.; Kennemur, J. L.; Bhethanabotla, V. C.; Ducharme, J.; Arnold, F. H. The β -subunit of tryptophan synthase is a latent tyrosine synthase. *Nat. Chem. Biol.* **2024**, 20 (8), 1086–1093.

(149) Zhou, H. S.; Meng, L. J.; Yin, X. J.; Liu, Y. Y.; Xu, G.; Wu, J. P.; Wu, M. B.; Yang, L. R. Artificial biocatalytic cascade with three enzymes in one pot for asymmetric synthesis of chiral unnatural amino acids. *Eur. J. Org. Chem.* **2019**, 2019 (38), 6470–6477.

(150) Parmeggiani, F.; Casamajo, A. R.; Colombo, D.; Ghezzi, M. C.; Galman, J. L.; Chica, R. A.; Brenna, E.; Turner, N. J. Biocatalytic retrosynthesis approaches to D-(2,4,5-trifluorophenyl)alanine, key precursor of the antidiabetic sitagliptin. *Green Chem.* **2019**, *21* (16), 4368–4379.

(151) Wang, B.; Zhou, J.; Zhang, X. Y.; Yang, Y. S.; Liu, C. H.; Zhu, H. L.; Jiao, Q. C. Covalently immobilize crude D-amino acid transaminase onto UiO-66-NH₂ surface for D-Ala biosynthesis. *Int. J. Biol. Macromol.* **2021**, *175*, 451–458.

(152) Miyata, A.; Chisuga, T.; Kambe, A.; Miyata, R.; Kawamura, Y.; Takeda, H.; Ito, S.; Nakano, S. Design of ancestral sortase E that is applicable in protein biomaterial synthesis. *ACS Catal.* **2024**, *14* (5), 3514–3523.

(153) Liu, G. J.; Wang, L. M.; Gao, Z. Y.; Feng, C. Q.; Liu, Q.; Chen, X. Q. Interfacially crystallized Enzyme@MOFs biocatalytic membranes for highly efficient synthesis of D-amino acids via continuously recirculating stereoinversion. *Chem. Eng. J.* **2024**, *497*, 154529.